

AN ABSTRACT OF THE THESIS OF


MIRCEA ION MANOLESCU for the degree MASTER OF SCIENCE  
(Name of student) (Degree)

in Mechanical Engineering presented on August 31, 1976  
(Major Department) (Date)

Title: A COMPARATIVE STUDY OF THE PERFORMANCE OF PIN FINNED  
HEAT SINKS FOR COOLING ELECTRONIC COMPONENTS BY NATURAL  
CONVECTION

*Redacted for Privacy*

Abstract Approved: \_\_\_\_\_

 (James R. Welty)

A study was conducted to determine the heat transfer characteristics of pin finned heat sinks in natural convection. Three pin diameters were studied: 0.238 cm, 0.318 cm and 0.396 cm. The pins were attached to the base in two arrangements, triangular and rectangular, forming a horizontal array. Pin spacing was parameterized by using pitch-to-diameter ratios of  $P/D = 2.0$ , 2.5 and 3.0 for each pin diameter.

This study presents information both for thermal design and heat transfer results. It was found that the largest spacing, rectangular pin arrangement and black anodized surface offered the

best power dissipation characteristics. The heat transfer results are presented in terms of the average Nusselt and Grashof numbers based on diameter. For Grashof numbers below 10 the data presented a variation characteristic of the behavior of small wires.

A comparison was made between a heat sink studied in this project and typical heat sinks with rectangular fins employed in the electronic industry. The pin finned heat sink displayed 46% and higher power densities than the ones with rectangular fins.

A Comparative Study of  
the Performance of Pin Finned Heat Sinks for  
Cooling Electronic Components by Natural Convection

by

Mircea Ion Manolescu

A THESIS

submitted to

Oregon State University

in partial fulfillment of  
the requirements for the  
degree of

Master of Science

June 1977

APPROVED:

*Redacted for Privacy*

---

Professor of Mechanical Engineering  
in charge of major

*Redacted for Privacy*

---

Head of Department of Mechanical Engineering

*Redacted for Privacy*

---

Dean of Graduate School

Date thesis is presented Aug. 31, 1976

Typed by Kathleen Manolescu for Mircea Ion Manolescu

## ACKNOWLEDGEMENTS

I now have the opportunity to thank those who have helped me transform this project into reality.

To Dr. James R. Welty for the always patient way of giving valuable advice and for constant understanding and encouragement

To Ed Meyer who took the photographs presented in this work

To Dave Churchill who performed some of the computational work

To Tektronix Inc. for providing the heat sinks and especially to Jack Hurt for his knowledgeable suggestions

To my friend and wife, Kathleen, who supported and understood me

To friends and colleagues for their good dispositions and understanding

## TABLE OF CONTENTS

<u>Chapter</u>		<u>Page</u>
I.	INTRODUCTION	1
II.	HEAT TRANSFER BACKGROUND AND LITERATURE REVIEW	8
	2.1 Background	8
	2.2 Vertical Flat Plate	12
	2.3 Horizontal Cylinders	17
	2.4 Heat Transfer From Fins	21
III.	DESIGN OF THE EXPERIMENT	24
	3.1 Apparatus	24
	3.1.1 Construction of the Heat Sinks	24
	3.1.2 Basic Test Section	27
	3.1.3. Additional Equipment	28
	3.2 Procedure	30
	3.3 Sources of Errors and Uncertainty Analysis	35
IV.	THERMAL DESIGN AND HEAT TRANSFER RESULTS	41
	4.1 Thermal Design	41
	4.2 Heat Transfer Results	48
V.	CONCLUSIONS AND RECOMMENDATIONS	68
	NOMENCLATURE	71
	BIBLIOGRAPHY	74
	APPENDIX A	78
	APPENDIX B	83
	APPENDIX C	86
	APPENDIX D	88

## LIST OF FIGURES

<u>Figure</u>		<u>Page</u>
I.1	Comparison Between the Effective Cooling Area of the Square Pins and Rectangular Fins	3
I.2	Cost Comparison Between Casting and Other Methods of Fabrication of the Heat Sinks	6
II.1	Coordinate System for a Vertical Surface and Typical Velocity and Temperature Profiles	13
III.1	View of the Heat Sinks	26
III.2	Photograph of the Heater Element	26
III.3	Close-up of the Assembled Heat Sink	29
III.4	View of the Test Set-up	29
III.5	Schematic of the Temperature Measurement Circuit	30
III.6	Sketch with Locations of Thermocouple Attachments	34
IV.1	Variation of Temperature Difference with Power Dissipated for $D = 0.238$ cm and a Black Anodized Surface	42
IV.2	Variation of Temperature Difference with Power Dissipated for $D = 0.318$ cm and a Black Anodized Surface	43
IV.3	Variation of Temperature Difference with Power Dissipated for $D = 0.396$ cm and a Black Anodized Surface	44
IV.4	Variation of Temperature Difference with Power Dissipated for $D = 0.238$ cm and a Polished Surface	45
IV.5	The Variation of the Power Dissipated with the Area-Volume Ratio for Black Anodized Surfaces	47
IV.6	The Variation of the Effective Thermal Resistance with $P/D$ for Rectangular Arrangement	50
IV.7	The Variation of the Effective Thermal Resistance with $P/D$ for Triangular Arrangement	51

<u>Figure</u>		<u>Page</u>
IV.8	Average Heat Transfer Results for $D = 0.238$ cm, Rectangular Pin Arrangement, Black Anodized Surface and $P/D = 2.0, 2.5$ and $3.0$	57
IV.9	Average Heat Transfer Results for $D = 0.318$ cm, Rectangular Pin Arrangement, Black Anodized Surface and $P/D = 2.0, 2.5$ and $3.0$	58
IV.10	Average Heat Transfer Results for $D = 0.396$ cm, Rectangular Pin Arrangement, Black Anodized Surface and $P/D = 2.0, 2.5$ and $3.0$	59
IV.11	Average Heat Transfer Results for $D = 0.238$ cm, Triangular Pin Arrangement, Black Anodized Surface and $P/D = 2.0, 2.5$ and $3.0$	60
IV.12	Average Heat Transfer Results for $D = 0.318$ cm, Triangular Pin Arrangement, Black Anodized Surface and $P/D = 2.0, 2.5$ and $3.0$	61
IV.13	Average Heat Transfer Results for $D = 0.396$ cm, Triangular Pin Arrangement, Black Anodized Surface and $P/D = 2.0, 2.5$ and $3.0$	62
IV.14	Comparison Between Rectangular and Triangular Pin Arrangements, Black and Polished Surfaces, for $D = 0.238$ cm and $P/D = 2.0$	64
IV.15	Comparison Between Rectangular and Triangular Pin Arrangements, Black and Polished Surfaces, for $D = 0.238$ cm and $P/D = 2.5$	65
IV.16	Comparison Between Rectangular and Triangular Pin Arrangements, Black and Polished Surfaces, for $D = 0.238$ cm and $P/D = 3.0$	66
A.1	Equivalent Thermal Circuit of the Heat Sink Assembly	78
A.2	Thermal Resistance of Interfaces as a Function of Contact Pressure	79
A.3	Model Representing the Clamp and the Support	80



## LIST OF TABLES

<u>Table</u>		<u>Page</u>
II.1	Comparison Between Ratios of Nusselt Numbers for Uniform Temperature and Uniform Heat Flux	16
III.1	Mnemonic Aid Referring to the Classification of the Heat Sinks	25

A COMPARATIVE STUDY OF  
THE PERFORMANCE OF PIN FINNED HEAT SINKS FOR  
COOLING ELECTRONIC COMPONENTS BY NATURAL CONVECTION

I. INTRODUCTION

From its early beginnings the electric and electronic industries have been faced with the problem of removing heat generated in systems and devices. Many components were emitting more thermal energy than their mass could dissipate; cooling therefore became a high priority problem. With the development of power transistors, high-current diodes, and, more recently, integrated circuits, cooling came to be one of the most critical problems to be solved.

Miniaturization, increased power densities, and high-reliability requirements have combined together to augment the necessity for careful thermal design and more efficient cooling devices. This constitutes the motivation of this work, which was initially prompted by the need for an efficient heat sink for the vertical preamplifier hybrid circuit which goes into the 455 Portable Oscilloscope manufactured by "Tektronix Inc." Besides being efficient this heat dissipator had to meet certain volume/weight requirements.

Several solutions are available for cooling electronic equipment, ranging from the simplest cases involving natural convection, to the more complicated ones involving evaporation and forced liquid cooling. Cooling by natural convection is by far the best method where volume/weight requirements become as important as the cooling process itself. This is especially true in the design of computers where cooling devices must be very efficient and, more importantly, small and light.

Cooling by natural convection implies air as the cooling medium and no other components (fans, blowers, pumps, etc.) in addition to the heat sink are required. This type of cooling is also dependent on the state of the air available and its temperature.

The majority of difficulties existing today in understanding and designing heat sinks lie in the "peculiar position" (1) that heat sinks hold in the electronic industry. They are in fact mechanical components, heat exchangers, yet their design is most often treated empirically, sometimes arbitrarily by the electronic designers.

Before proceeding further, it would be worthwhile discussing some of the more important aspects involved in heat sink design. First, the goal in designing heat sinks for electronic equipment can be formulated in either of the following ways: to hold the transmitted power constant and to reduce the temperature difference between the hot surface and surroundings, or to maintain a fixed temperature difference between the electronic component and ambient and to increase the power dissipated.

The rate at which heat is dissipated by convection from a heated surface is equal to the product between the area in contact with the surrounding fluid, the average temperature difference between surface and fluid, and the heat transfer coefficient. Since the temperature difference is a fixed quantity there are two obvious ways to increase heat transfer.

One way to increase the heat transfer rate out of the element would be to increase the heat transfer coefficient. This may be accomplished, for example, by increasing the velocity of the fluid

flowing past the system (forced convection). That would be done at the expense of space since a twofold increase in heat transfer coefficient requires more than a twofold increase in fluid velocity or an almost fourfold increase in pressure loss and possibly an eightfold increase in the power requirements (2). The outcome would imply use of pumps, piping, etc., and the design would become bulky and expensive.

The other way of improving cooling is to increase the heat transfer surface area, that is, by adding extended surfaces. The shape of these could be rectangular (longitudinal fins), disk-like (circular or radial fins) or cylindrical (pin fins or spines), etc. The latter has superior heat transfer characteristics over the others (3, 4, 1). Pin fins promote turbulence and the airflow can be either in the plane of the array or perpendicular to it. Also, the effective cooling area for pin fins is greater than the one for rectangular fins. Refer to Figure I.1.

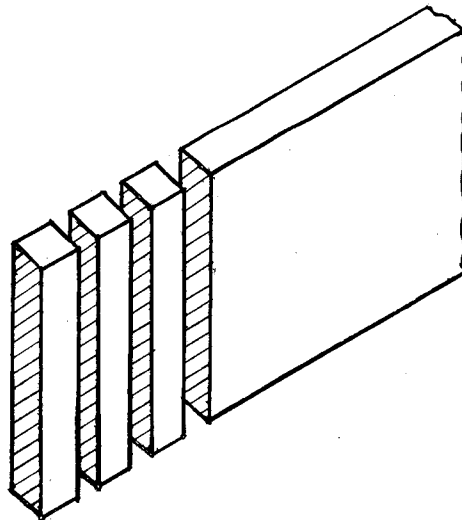


Figure I.1  
Comparison Between the Effective Cooling Area of  
the Square Pins and Rectangular Fins

Fin spacing has a great influence upon the heat transfer characteristics of a heat sink. Fins should be close enough to each other to yield a compact design (maximum heat transfer area for a given volume), but separated far enough such that neighboring fins will not impair the airflow or that their overlapping boundary layers would interfere to the extent of drastically altering the performance of the heat sink. More about this subject will follow in the section treating the heat transfer results.

In order to ensure a minimum resistance to the flow of thermal energy through the heat sink, all thermal contacts between different components of the heat sink or between the heat sink and the electronic components to be attached to it must also have the minimum attainable thermal resistance. This can be achieved by assembling the respective parts under pressure and using special thermal joint compounds, or by brazing or soldering the components together where feasible.

Factors affecting thermal design have been presented thus far. Since mechanical and economic considerations are also important in heat sink design, they will be considered next.

The choice of materials for heat sinks is usually narrowed down to a few: diamond, silver, copper, beryllium oxide, aluminum, and steel. They are listed in order of decreasing thermal conductivity and cost. Indeed, diamond has the best thermal conductivity of all materials, but its high cost prohibits its use in common applications. It is used only in space applications or high power devices. Silver presents the same situation. Copper is a very good thermal conductor. It has twice the thermal conductivity of aluminum, but weighs three times more than

aluminum. The cost per unit weight of copper is also greater than that of aluminum (one and one half times). Beryllium oxide is also an excellent though expensive conductor. Steel is used for high pressure applications. From the point of view of machinability, both copper and aluminum present good characteristics. In light of the above discussion, aluminum emerges as being the favorite choice; this is reflected in today's heat sink market.

A device worth mentioning is the heat pipe. Its outstanding thermal capabilities are due to two phenomena: capillarity and change of phase. Size considerations (5, p. 39), however, bar its use in applications involving small available spaces.

Component accessibility and surface finish are two other important factors in a sound mechanical and thermal design of heat sinks. The surface can be polished, painted, etc., in this way influencing the radiative heat transfer capabilities.

Perhaps the most important factor overall is the cost of fabrication. Of all methods, the most commonly employed is extrusion. It recovers its relatively high initial cost after a small number of pieces are fabricated. The shapes produced are, however, limited. Stamping is a very good and cheap method of fabrication when the powers to be dissipated by the heat sinks are low and the thickness of the sheet of metal used does not exceed 0.23 cm (1). Finally, die cast heat sinks offer a great flexibility in obtaining a diversity of shapes but the method requires generally a greater number of pieces fabricated in order to become economically feasible. For the purpose of illustration a comparison between different methods of casting, extrusion and

machining can be made, using a compilation published in Metals Handbook (6, p. 874-891). It appears that the break even point for fabricating a component of relatively simple geometry, except the casted part which is more complicated, is about 1,400 parts/day if the comparison is

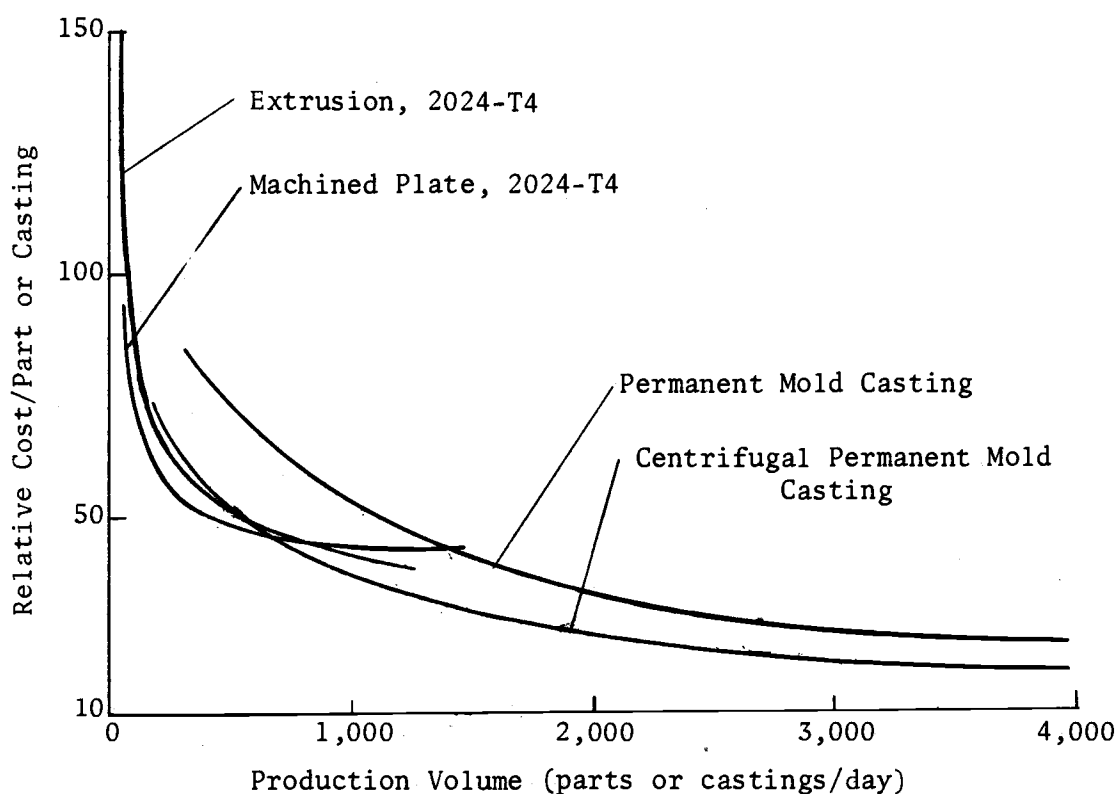


Figure I.2  
Cost Comparison Between Casting and Other Methods of Fabrication  
Of the Heat Sinks

made between machined and permanent mold casting, and about 500 parts/day if extrusion is compared with a centrifugal permanent mold. Thus, if a large number of parts is desired, casting can be advantageous. Of course these numbers are only estimates and they vary with

complexity of the parts, etc.

Three important points should be made regarding the design and fabrication of heat sinks. One is that, unless the volume of production of the heat sinks is high, extruded and impact extruded (stamped) heat sinks are least expensive. The other two observations are related to what a good heat sink design actually means: a maximum surface area/unit volume ratio and a minimum temperature difference across the heat sink.



## II. HEAT TRANSFER CONSIDERATIONS AND LITERATURE REVIEW

### 2.1. Background

It is the purpose of this chapter to present some of the more important concepts and definitions of heat transfer related to this work and a short literature review dealing with free convection heat transfer from vertical flat plates, single and bundles of horizontal cylinders, and from extended surfaces to air.

Conduction is characteristic to transmission of heat through solids. The driving force of the heat flow is the temperature difference between two given locations within a solid. Heat transfer rate is given by the Fourier's first law of heat conduction,

$$\vec{q}' = -k\nabla T \quad (2.1)$$

where  $k$  is the proportional constant between the heat flux vector and the temperature gradient. It is called thermal conductivity and a good discussion of it and references are presented by Welty, Wicks and Wilson (7). An analogy between the electric and heat transfer systems is helpful for calculation purposes. Ohm's law has a counterpart in heat transfer which is given as follows:

$$q = \frac{\Delta T}{\Sigma R} \quad (2.2)$$

Heat transfer rate  $q$ , similar to the electric current, is equal to the quotient between the temperature difference  $\Delta T$  and the equivalent

thermal resistance which is similar to the quotient between the electric potential difference and the equivalent electric resistance respectively. The equivalent resistance can be the sum of several resistances in parallel or series. For a plane wall Equation 2.2 can be written as:

$$q = \frac{\Delta T}{L/kA} \quad (2.3)$$

It is important to mention that in the above discussion, as in this entire work, steady-state conditions are assumed, that is, no variations with time are present.

Radiation heat transfer contrasts sharply from the other modes of heat transfer since it does not require a medium of propagation. In fact, the heat transferred by radiation is maximum in a perfect vacuum. The nature of thermal radiation is electromagnetic and is thus governed by the laws of wave mechanics. The Stefan-Boltzmann law for a blackbody (perfect emitter) total emissive power is:

$$E_b = \sigma T^4 \quad (2.4)$$

where  $\sigma$  is Stefan Boltzman constant,  $\sigma = 5.6699 \times 10^{-12} \text{ Watt/cm}^2 \text{ } ^\circ\text{K}^4$ .

Most surfaces do not behave as ideal black surfaces and their total emissive power is different by a proportionality constant called emissivity,  $\epsilon$ . The net radiation between two such gray surfaces is:

$$q_{1-2} = A_1 \Omega_{1-2} (E_{b_1} - E_{b_2}) \quad (2.5)$$

where  $\Omega_{1-2}$ , the shape factor for diffuse radiation between two gray

surfaces is given by:

$$\Omega_{1-2} = \frac{1}{\frac{(1-\epsilon_1)/\epsilon_1}{1} + \frac{1/F_{1-2}}{1} + \frac{(A_1/A_2)(1-\epsilon_2)/\epsilon_2}{2}} \quad (2.6)$$

In the above equation  $F_{1-2}$  is the shape factor for radiative exchange between two given bodies. Radiation contribution in this experiment is expected to be small since the temperature differences involved are small.

Heat transfer by convection is concerned with the exchange between a surface and an adjacent fluid. The heat flow rate is given by the Newton rate equation:

$$q = hA\Delta T \quad (2.7)$$

If the adjacent fluid is made to flow by external means such as a blower or a pump, convection is called forced as opposed to free convection in which the motion of the fluid is caused by the interaction of a difference in density with the gravitational field.

The dimensionless parameters characteristic to natural convection for the case of laminar flow and for which inertia forces are negligible compared to friction and buoyancy forces are related in the following way:

$$Nu = C \cdot (GrPr)^{1/4} \quad (2.8)$$

In an excellent paper by Hellums and Churchill (8) a complete analysis is presented for obtaining meaningful dimensionless groups and the

relations between them from the continuity, momentum, and energy equations. The Grashof number,  $Gr$ , is the ratio of the body forces to viscous forces and its value indicates whether the flow is laminar or turbulent.

A very important concept in convection is the one of boundary layer. When fluid flows over a plate, for example, its velocity varies with the distance from the plate. At the surface the velocity is zero, reaching a value  $v_{\infty}$  at a certain distance from the plate. The velocity  $v_{\infty}$  is called the free stream velocity and it remains unchanged at locations outside the boundary layer.

The region in which the velocity gradient is different from zero is called the hydrodynamic boundary layer. Velocity gradient becomes zero at a distance  $\delta$  from the surface which is called boundary layer thickness. At the leading edge of the plate the thickness of the boundary layer is zero and the flow inside the boundary layer is always laminar (layers of fluid moving past one another with no bulk movement of particles between them), regardless of the free stream conditions. The hydrodynamic boundary layer has a counterpart in heat transfer, the thermal boundary layer. It is postulated that thermal energy is transferred by conduction across the laminar boundary layer. The conductive resistance of the laminar film is the controlling factor in the convective processes.

Since Prandtl number is a ratio of the momentum diffusivity to the thermal diffusivity, it is an indication of how soon the thermal boundary layer develops in respect to the hydrodynamic one. For a Prandtl number of unity the thermal and hydrodynamic boundary layers

develop simultaneously. This is the case with air which approximates well this situation ( $Pr \approx 0.7$ ).

It is rare when heat transfer occurs by one mode only. Usually a combination of them is present, such as in this work where natural convection occurs simultaneously with radiation at the surface and conduction occurs along the pins. The expression which gives the heat exchange rate by convection (Equation 2.5), can be linearized (9) and combined with Equation 2.7 to obtain a combined coefficient of heat transfer. This procedure is illustrated in Appendix C. The heat transfer coefficient used in Nusselt number calculations in this work includes the radiation contribution.

The geometry of the heat sinks studied in this research is a combination of a vertical flat plate and horizontal cylinders. It is thus beneficial to review briefly the heat transfer literature dealing with these geometries.

## 2.2. Vertical Flat Plate

The case of heat transfer by natural convection from a heated vertical flat surface to an adjacent still fluid is frequently encountered and numerous excellent studies, both analytical and experimental, have been conducted on this geometry. The fluid is assumed to be of infinite extent and free of any motion other than that associated with natural convection near the heated wall.

Early analytical work was concerned with the so called "classical problem of the flat plate". The assumptions involved in it were: laminar steady flow; uniform surface temperature; properties of the

fluid except density unaffected by temperature; no heat sources within the fluid; and negligible viscous dissipation. Two methods of analysis are available. One is to solve the differential equations making use of similarity transformations, and the other is to obtain solutions in integral form, assuming temperature and velocity profiles.

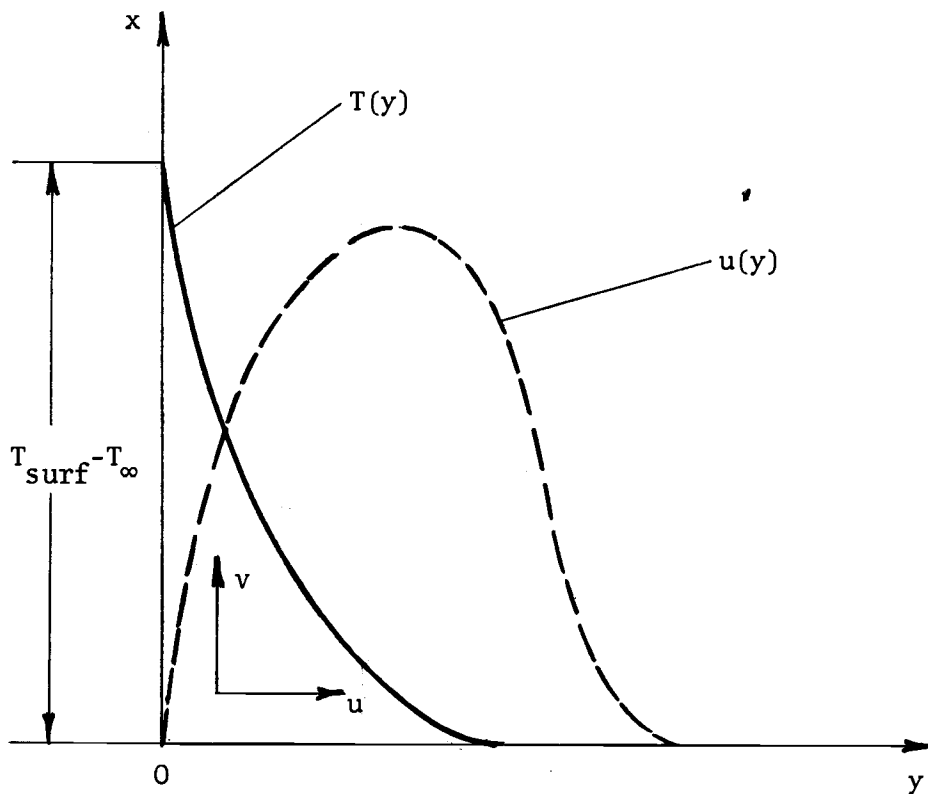


Figure II.1. Coordinate System for a Vertical Surface and Typical Velocity and Temperature Profiles in Natural Convection

In 1881 Lorenz [reported in Ede (10)] simplified and solved the governing differential equations and obtained:

$$\text{Nu}_L = 0.548 (\text{Gr}_L \text{Pr})^{1/4}$$

Although this equation is in good agreement with experimental data, it

was assumed that no variation occurred in the x direction<sup>1</sup> regarding velocity and temperature profiles; this is certainly not the case.

Schmidt and Beckmann (11) solved in 1930 the differential equations of continuity, momentum, and energy in which the boundary layer assumptions were made. Using the method of similarity transformation Pohlhausen (12) transformed the differential equations to a set of ordinary differential equations and tried to obtain a series solution. Due to the slow convergence of the series he was forced to use Schmidt and Beckmann's experimental values for some boundary conditions and obtained numerically a solution for the specific case of  $Pr = 0.733$ .

$$Nu_L = 0.52 (Gr_L Pr)^{1/4}$$

Studies conducted by Saunders in 1939 (13) and in 1948 by Schuh were aimed at obtaining further solutions of the same differential equations. Saunders' study had two parts: an analytical one, in which he approximated the temperature variation in the boundary layer with high order polynomials, and an experimental one by which he backed his results. His results are in the form:

$$Nu_L = f(Pr) (Gr_L Pr)^{1/4}$$

He used air, water and mercury as fluids.

Using an integral technique Eckert (14) obtained the following expression for the local Nusselt number for an isothermal vertical flat

---

<sup>1</sup> Figure II.1 shows the system of coordinates employed in natural convection analysis and typical temperature and velocity profiles.

plate:

$$Nu_x = 0.508 Pr^{1/2} (0.952 + Pr)^{-1/4} (Gr_x)^{1/4}$$

He assumed in his analysis parabolic velocity and temperature profiles. By a simple integration Eckert found that "the average heat transfer coefficient of a vertical plate with a height  $x$  is  $4/3$  the local value at the point  $x$ " (14, p. 158). When the medium is air with a Prandtl number of 0.714 the following is obtained:

$$Nu_x = 0.378 (Gr_x)^{1/4}$$

The coefficient 0.378 yields a five percent relative error when compared with 0.360, the coefficient resulted from Schmidt and Beckmann's more exact analysis.

Ostrach (15) obtained exact computer solutions for eight values of Prandtl number ranging from 0.01 to 1,000, air included. He assumed in his analysis that the temperature differences between wall and ambient fluid are small and made use of the boundary layer approximations and similarity technique. His results are given below:

$$Nu_x = (3/4) f(Pr) (Gr_x)^{1/4}$$

$$Nu_L = f(Pr) (Gr_L)^{1/4}$$

Values for  $f(Pr)$  are also given in the study.

Other authors performed calculations adding more values of  $f(Pr)$



to the ones found by Ostrach. The interested reader can find these references in (10, p. 7). Ostrach practically completed the classical problem with his study.

An analytical solution for the variable surface temperature and wall heat flux was given for different values of Pr number by Sparrow (16) in 1955. His analysis employed the approximate Karman-Pohlhausen integral technique and a solution was obtained by a series expansion. For the case of constant wall temperature, Sparrow's results are the same as Eckert's published in (14). Sparrow and Gregg (17) developed a similarity solution for the case of uniform surface heat flux. Results for four Prandtl numbers were obtained by computer. It is interesting to observe that the mean Nusselt numbers for the uniform surface heat flux case were found to be very close (higher) to those for the uniform temperature case. Two different Nusselt numbers were used; one in which an average temperature difference for the whole plate was used, and another in which the temperature difference was evaluated at one-half of the total height of the plate. Table II.1. presents a comparison between the cases of uniform temperature and heat flux for both "mean" and "halfway" Nusselt numbers.

Table II.1. Comparison Between Ratios of Nusselt Numbers for Uniform Temperature and Uniform Heat Flux

Pr	Ratios of "Mean" Nusselt Numbers	Ratios of "Halfway" Nusselt Numbers
0.1	1.08	1.02
1	1.07	1.015
10	1.06	1.01
100	1.05	1.00

Thus for fluids having high Prandtl numbers the cases for uniform heat flux and surface temperature are identical.

This review of natural heat transfer from vertical flat surfaces in the laminar regime is by no means exhaustive. Excellent surveys (10, 18) dealing with this and other geometries can furnish the interested reader with a more complete picture.

### 2.3. Horizontal Cylinders

The problem of heat transfer from horizontal cylinders under natural convection is one of considerable practical importance. Several investigators have conducted studies on this geometry using both analytical and experimental methods.

In his paper Hermann (19) started his analysis from the Navier-Stokes and the Fourier-Poisson equations, assuming that the boundary layer thickness was small compared with the diameter of the cylinder. He obtained the following form  $Nu_D \sim Gr_D^{1/4}$  which generalized gives  $Nu_D \sim C (Gr_D Pr_D)^{1/4}$ , a familiar result. His results are in good agreement with the ones obtained in 1933 by Jodlbauer (20). Jodlbauer measured the velocity and temperature profiles for a cylinder 5.0 cm in diameter under natural convection. He took the measurements in air at atmospheric pressure using an anemometer and thermocouples. His results show basically that the average heat transfer coefficient of a horizontal cylinder of diameter  $D$  is equivalent to the average heat transfer coefficient of a vertical wall of height  $2.5D$ .

From schlieren photographs it was deduced that Hermann's results hold for  $10^4 < Gr_D Pr_D < 10^8$ . For  $Gr_D Pr_D < 10^4$  they fail since the boundary

layer thickness is significant when compared with the diameter of a thin wire.

In 1912 Langmuir (21) had suggested in his "film theory" that the boundary layer be idealized as being a stationary cylindrical air layer around the wire. The thermal energy given off through this layer would be solely by conduction. He found also that for very small wires the rate of heat dissipation is independent of diameter. In a series of two articles Rice (22, 23) applied Langmuir's "film theory" and found the following relation for the Nusselt number:

$$Nu_D = \frac{2}{\ln\left[1 + \frac{2}{0.47(Gr_D Pr)^{1/4}}\right]}$$

This result follows the trend of the experimental data. For  $GrPr < 10$ , however, the agreement is not very good.

Following the ideas of Langmuir and Rice, Eckert (14) found for thin wires in air:

$$Nu_D = \frac{2}{\ln\left[1 + \frac{2}{0.400(Gr_D)^{1/4}}\right]}$$

which is said to be in excellent agreement with the experimental results.

King (24) and later McAdams (25) found empirical interpolation curves and McAdams also compared these curves with the work done by other investigators between 1892 and 1939. Their curves fit experi-

mental data well for the range  $10^4 < Gr_D Pr < 10^8$ . It is interesting to mention the fact that in 1942 Mueller (26) found excellent agreement between his results for vertical wires and the line recommended by McAdams for horizontal wires.

In a report written in 1948 (4) and in a simplified form of this (27) published the same year, Elenbaas found by applying Langmuir's concept of fictitious film a relationship valid for all fluids:

$$Nu_D^3 e^{-6/Nu} = \frac{Gr_D Pr}{f(Gr_D Pr)}$$

The function of  $f(Gr_D Pr)$  was found by experiment to be 1 for  $Gr_D Pr < 10^4$ . The above equation is in excellent agreement with data for air, hydrogen, water, mercury, carbon dioxide, etc. Senftleben [reported in (25)] continued the efforts of his predecessors and obtained an expression for the average Nusselt number as a function of the thickness of the conduction layer. He combined in his analysis Langmuir's film concept with the hydrodynamic theory of viscous flow. For the range  $10^{-1} < Gr_D Pr < 10^4$  he obtains identical results with Elenbaas. In his book, Hsu (29) gives a relationship which applies for the case of streamline flow in natural convection of both metallic and nonmetallic fluids adjacent to horizontal cylinders larger than wires:

$$Nu_D = 0.53 \left( \frac{Pr}{Pr + 0.952} Gr_D Pr \right)^{1/4}$$

He also gives the point of transition to turbulent flow for nonmetallic fluids to occur at:

$$\text{Gr}_D \text{Pr} = D^3 \times 10^{11.2 \pm 0.2}$$

Hsu further observed that the heat transfer coefficient is not affected by the wetting capabilities of a clean surface.

An extensive survey was conducted by Van de Hegge Zijnen (28) in 1956. He experimented with platinum wires and brass cylinders in air and obtained correlations for predicting heat transfer from horizontal cylinders to air by combined forced and natural convection. These correlations eventually yielded the values of Reynolds number above which natural convection is negligible. An attempt to obtain velocity and temperature profiles was made by Sesonske (30) who took temperature measurements at the midsection of a cylinder. An optical method for measuring the velocity is also presented.

Recently Nakai (31) wrote a two-part article dealing with the theoretical and experimental aspects of pure natural and forced convection. A combination of the two at low Reynolds and Grashof numbers is also studied.

This concludes the literature review of natural convection heat transfer in laminar flow from horizontal cylinders. The work done in this area is extensive in contrast with the studies of natural convection from bundles of horizontal cylinders. This writer found a single article on this subject dealing with an interferometric study by Eckert and Soehngen, referenced by Holman (32) and by Hsu (29).

A short study of the literature published concerning natural convection heat transfer from fins to air follows next.

#### 2.4. Heat Transfer From Fins

This section will present some of the ideas and developments found in the literature dealing with heat transfer from fin arrays.

Conduction through fins is the best understood aspect of the heat transfer from extended surfaces. Natural convection and radiation heat transfer from fins are not as well documented, especially when they occur simultaneously, as is usually the case. The paper that apparently was first to solve the nonlinear differential equation resulting from the combined heat transfer from cylindrical fins was published in 1963 by Cobble (33). Cobble started with the differential equation governing the steady state heat transfer by conduction, convection, and radiation for a cylindrical fin:

$$\frac{d^2T}{dx^2} - \frac{hP}{kA}(T-T_{\infty}) - \frac{\sigma \epsilon P}{kA}(T^4-T_{\infty}^4) = 0 \quad (2.9)$$

He used an empirical relationship for the natural convection heat transfer coefficient, then grouped the nonlinear terms in a function  $F(t)$  and developed an equivalent function  $U(t)$  by using a forward interpolation technique. He then integrated the differential equation twice obtaining an integral equation, giving finally the temperature distribution in terms of elliptic functions. An experiment with a 2.54 centimeter diameter aluminum fin was performed to supplement the theoretical work and the agreement was found to be good. One merit of Cobble's study was that it demonstrated the need

to account for convection and radiation and it provided an expression for the temperature distribution for this case. Two years later Collicot (34) conducted a nearly identical study using a Runge-Kutta technique to solve the dimensionless nonlinear differential equation. Edwards and Chaddock (35) experimented with cylindrical disk fins for different spacings and found that for fins with high thermal conductivity, fin diameter did not play a significant role in the heat transfer. They also developed a modified Nusselt number,  $Nu_p$ , based on spacing, and observed that at modified Raleigh numbers between 100-500 the slope of the line generated by plotting  $Nu_p$  versus  $Ra_p$  on log-log coordinates was not one-fourth. Similar results are presented by Pan and Knudsen (36). Both papers attributed this to severe interference between the velocity boundary layers. To account for this, Edwards and Chaddock derived separate empirical equations for their data, representing the boundary layer regions both with interference and noninterference respectively.

Dusinberre (37) made a useful contribution to the field of extended surface heat transfer by developing an expression for the heat transfer film coefficient of fins from an "effective" expression that is obtained through measurements from a system composed of the fin array and base plate. His expression for the "local" heat transfer coefficient is:

$$h = \{[(1-Ch')^2 + 4BCh']^{1/2} - (1-Ch')\} / 2BC \quad (2.10)$$

where  $B = \frac{A_b}{A}$  and for a cylindrical pin  $C = L^2 P / 3kA_s$ . The notation used is given in the nomenclature.

A few other studies should be mentioned in addition to the ones already presented. Starner and McManus (38) described a study said to be the first to include in their experimental set up a metal base attached to a vertical array of rectangular fins, which very much resembles a heat sink. Their results are found to be 10-20% below the results obtained by Elenbaas for the parallel plates geometry. Their findings are confirmed by the work of Welling and Wooldridge (39) in 1965. The same geometry was studied in 1967 by Harahap and McManus (40) "because of the scarcity of data for heat transfer from fins in the horizontal orientation" (40, p. 35). These authors generalized their data by finding new dimensionless groups accounting for the influence of fin spacing. They also used an averaged temperature over the base and fin and studied the flow field patterns by using a schlieren technique.

This short review cannot be concluded without mentioning the only experimental study of pin fins (3) found by this writer. The author, Werner Drexell, is in fact more interested in forced convection over an array of vertical cylindrical and square pins. He made some important observations, however, one of them being that the heat transfer coefficient increases as the diameter of the pins decreases.

It appears that the heat sink geometry studied in this research has not been studied previously. Whenever possible, parallels between the results obtained in this study and similar studies will be made. Conclusions and inferences will be drawn where possible, also.

For a good bibliography of heat transfer from extended surfaces, the interested reader should consult Bergles (41).



### III. DESIGN OF THE EXPERIMENT

#### 3.1. Apparatus

##### 3.1.1. Construction of the Heat Sinks

The principal concerns of heat sink design were the limited space available and the desired high efficiency of the device. The choice of overall dimensions was based on guidelines provided by Tektronix Inc. They are comparable with the ones used in the electronic industry today. Pin fins were chosen as the extended surfaces in an attempt to show that they are more efficient than rectangular fins. Initially it was intended that the heat sinks would be made of one piece, but the high cost involved forced this idea to be abandoned.

The base was made from a sheet of 50-52 aluminum alloy, with a square base measuring 4.445 cm and with a thickness of 0.318 cm. Tolerances were measured to be  $\pm 0.005$  cm and  $\pm 0.01$  cm respectively. Cylindrical spines made of 20-11 aluminum alloy were press-fitted in holes drilled in the base.<sup>2</sup> The spines were measured to be 2.225 cm in length with tolerances of  $\pm 0.005$  cm. The portion of the spine above the surface of the base, that is, in contact with the ambient air, had a measured length of  $1.908 \pm 0.01$  cm. Three spine diameters were used in this work: 0.396 cm, 0.318 cm and 0.238 cm respectively. The measured tolerances for the first two were 0.003 cm and 0.001 cm

---

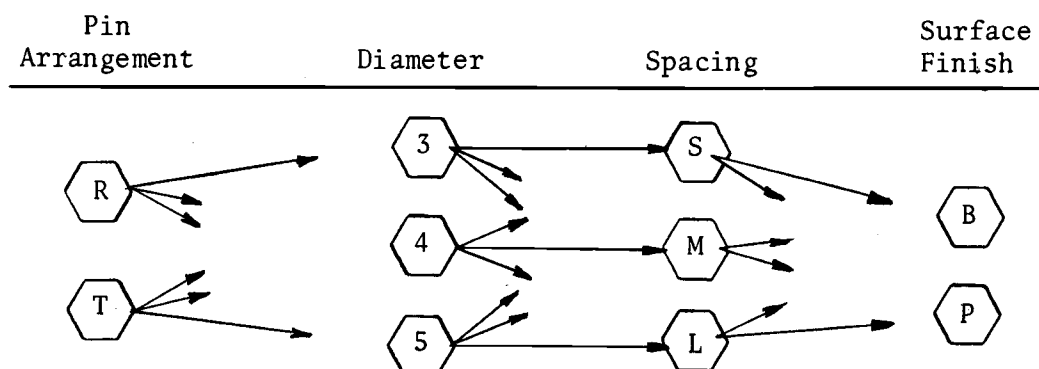
<sup>2</sup>Both 50-52 and 20-11 aluminum alloys have a lower thermal conductivity than pure aluminum, but they were preferred for their machinability and strength. The electronic industry currently makes use of similar aluminum alloys.

for the third.

The pin arrays consisted of two patterns: rectangular and equilateral triangular. For each diameter pitch-to-diameter ratios of 2.0, 2.5 and 3.0 were used, requiring that 18 heat sink units be tested. The heat sinks were first utilized with their surfaces polished, then they were black anodized in order to enhance heat transfer by radiation. Three of these heat sinks can be seen in Figure III.1.

To distinguish the various combinations of geometry, P/D, surface finish, and diameter, a special nomenclature was developed. According to this nomenclature one character would be a number (3, 4, or 5) which would represent the diameter of the pins of the respective heat sink in thirty-seconds of an inch. Another character would be either S, M or L, indicating the words "small", "medium" and "large" and referring to fin spacing (P/D). Positioning of the pin in a triangular or rectangular pattern suggested the letters T or R as a third character. The last character refers to the type of finish of the surface. Polished and black anodized surfaces were

Table III.1. Mnemonic Aid Referring to the Classification of the Heat Sinks



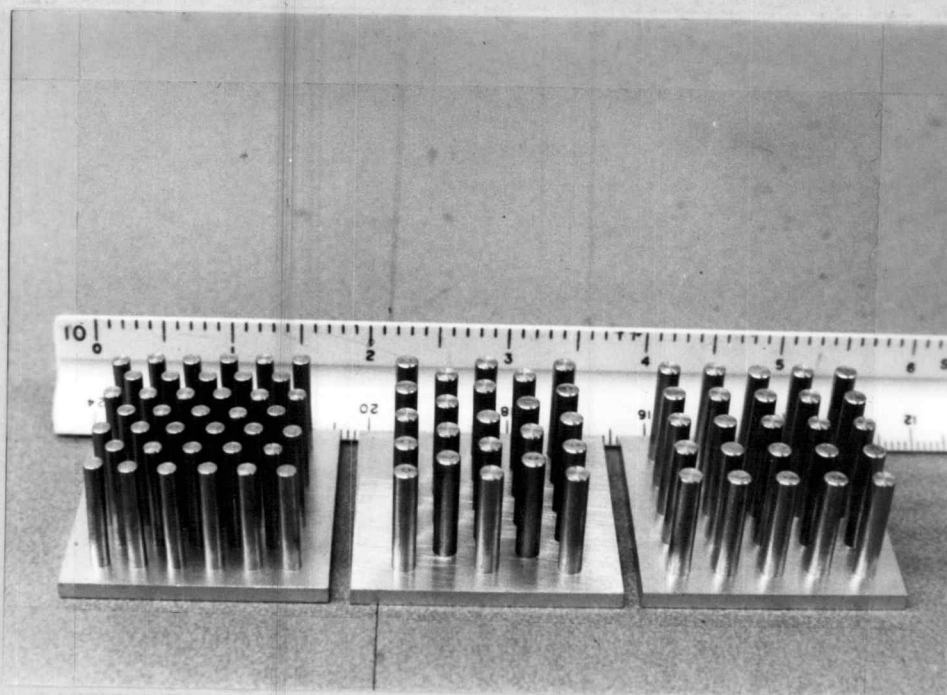


Figure III.1. View of the Heat Sinks

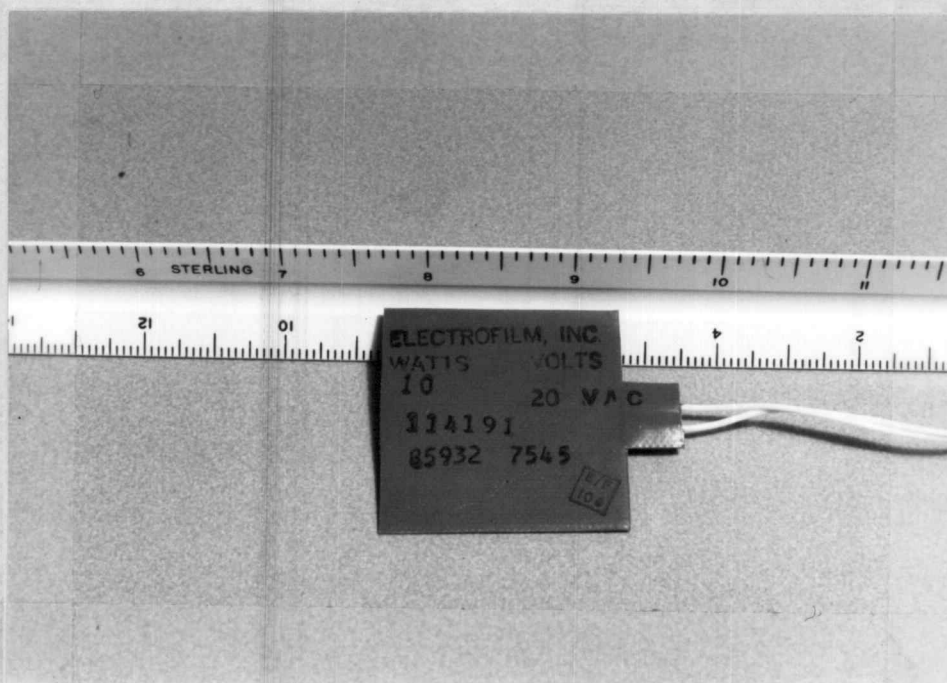


Figure III.2. Photograph of the Heater Element

designated P and B. For a good mnemonic aid, refer to Table III.1.

### 3.1.2. Basic Test Section

The heat sinks were positioned during the tests with the base vertical, therefore the pins formed a horizontal array. Proper positioning of the heat sinks was checked at the beginning of each run with a level. Considerable simplification of the treatment of data was achieved by creating a "sandwich" made up of two identical heat sinks, back to back, with a heater element situated between them. This ensured that an equal amount of heat was dissipated in both directions. A close-up picture of the assembled heat sink is presented in Figure III.3.

The heater element was made by Electrofilm Inc.; it consisted of two identical chemically etched resistance circuits separated by insulation and bonded at the exterior by fiberglass reinforced silicone rubber layers. The heater measured 4.128 by 4.128 cm with an unheated tab of 1.276 by 0.943 cm from which emerged Teflon-insulated lead wires. Nominal thickness of the heated portion of the heater was 0.068 cm and that of the tab 0.148 cm. A photograph of the heater element can be seen in Figure III.2. The heater was rated 10 Watts at 20 VAC. The fact that the area of the heater was smaller than the area of the base of the heat sink was not considered to have a significant influence upon the data. Aluminum, being a good conductor, tended to distribute heat uniformly across the base, minimizing temperature variations.

The heat sink-heater "sandwich" was supported by a simple device consisting of two steel clamps fitting in two bent steel tubes

attached to two adjustable supports [ D <sup>3</sup> ]. The heat sinks were in position at about 180 cm above the floor. See Figure III.4.

### 3.1.3. Additional Equipment

A general view of the experimental set-up is given in Figure III.4. Input in the system was provided by a Regulated Power Supply, Model 810B made by Harrison Laboratories Inc. The rated maximum output was 450 Watts. The power supply was not included in the picture of the equipment arrangement. Power supplied to the heater was determined by taking the product between voltage and current that passed through the leads of the heater.

A Fluke 8200A Digital Voltmeter [A] was used for voltage measurement. The accuracy of the instrument was  $\pm 0.05\%$ . Current was measured with a Keithley 160B Digital Multimeter [B] capable of measurements within one nano Ampere. The specified accuracy of this instrument was  $\pm 0.1\%$ . No drift was detected for the Keithley Digital Multimeter; a drift of 0.027% was recorded for the Fluke Digital Voltmeter, which was quite acceptable.

Temperature was measured at several locations on the surface of the heat sinks by means of iron-constantan thermocouples. Ambient temperature was measured using the same kind of thermocouple. Due to the good quality of the thermocouple wires (42), no attempt was made to calibrate them. The reference tables for iron-constantan thermocouples were used to obtain temperature values from the corresponding emf readings. The thermocouples were connected through a switch box [C]

---

<sup>3</sup> Letters in brackets correspond to equipment shown in Figure III.4.

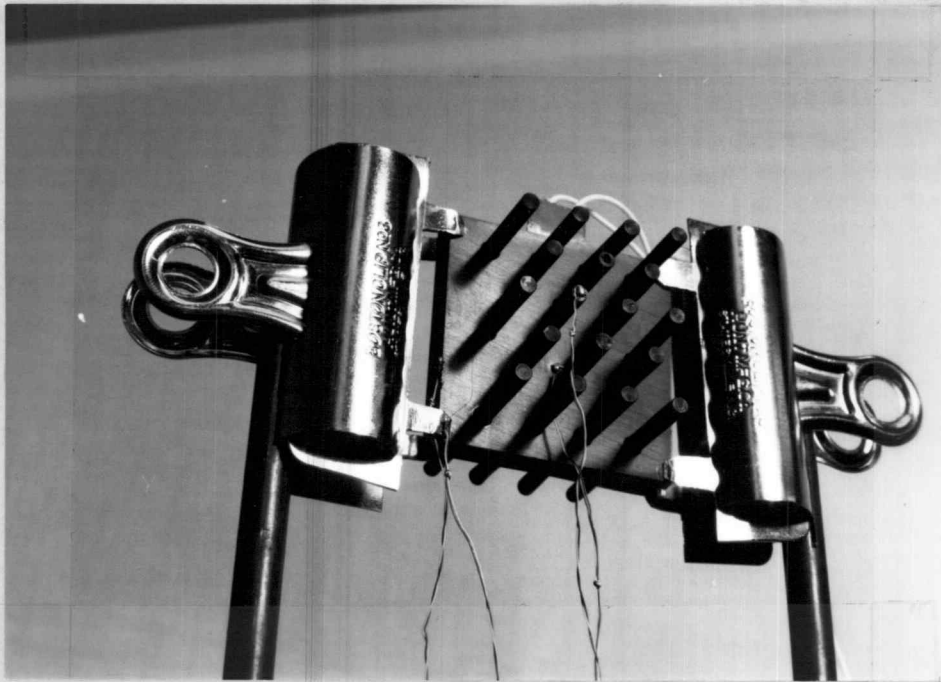


Figure III.3. Close-up of the Assembled Heat Sink

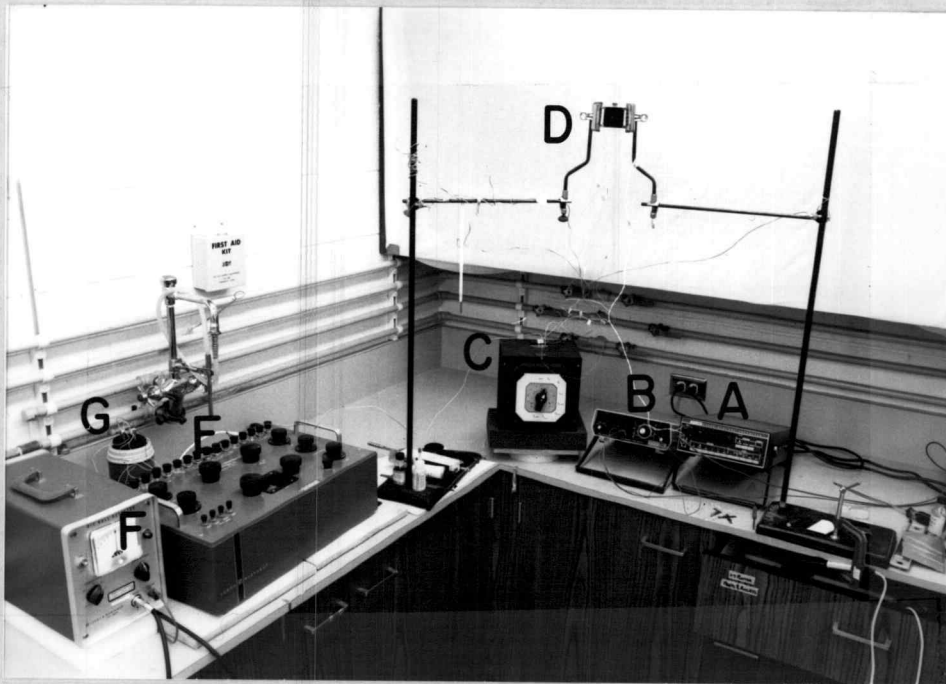


Figure III.4. View of the Test Set-up

to the ice bath cold junction [G]. Two copper extension leads provided the connection between the cold junction and a 7553 model of the K-3 Universal Potentiometer [E] manufactured by Leeds & Northrup Co. This device had a specified accuracy of  $\pm 0.5 \mu\text{V}$  or approximately

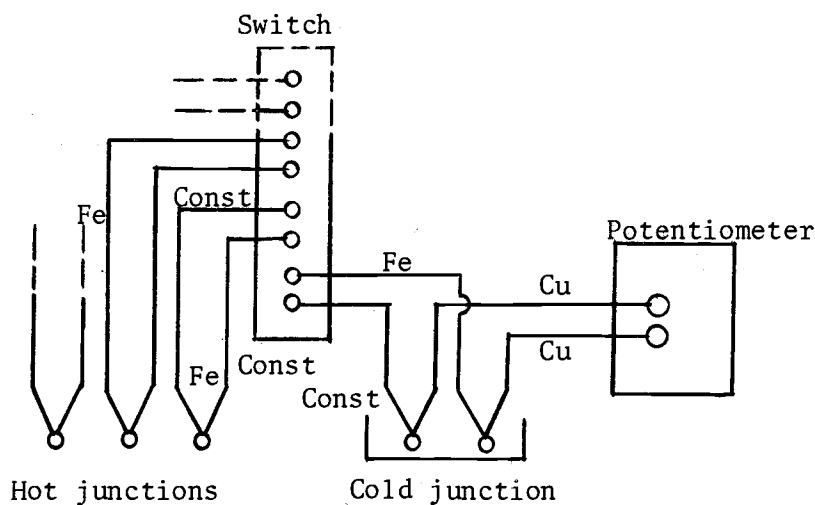


Figure III.5. Schematic of the Temperature Measurement Circuit

$\pm 0.01^\circ\text{C}$ . A DC Null Detector manufactured by the same company was used in conjunction with the potentiometer. Auxiliary equipment used with the potentiometer were the 3 Volt-DC constant voltage supply and an Eppley standard cell. A schematic of the temperature measurement circuit is given in Figure III.5.

### 3.2. Procedure

Eighteen different heat sink designs, resulting from the combination of different fin arrangements, were tested; values for power

and temperature were obtained for each case. The surface of the heat sinks was polished for the first set of runs and had an emissivity of between 0.05 and 0.13 (43, 35 and 44). The surface was black anodized for the second set of runs with an emissivity somewhere between 0.8 and 0.95 (43, p. 49).

Prior to a run it was necessary to make two kinds of preparations, one related to the heat sink assembly and one to the measuring equipment. The heat sinks were first cleaned of dirt particles with a water jet, then placed in a solution of acetone to remove grease, etc. Holes had previously been drilled on the side of the base and axially on the tip of the pin situated closest to the middle of the heat sink. This was done to accommodate the thermocouple hot junctions. The holes were then filled with silicone grease in order to decrease the thermal resistance. This method was abandoned when some inconsistencies in surface temperature data were encountered. In the new method the thermocouple bead was soldered to a small square copper tape which had an adhesive substance on the back. This was pressed onto the surface whose temperature was desired. This method provided a superior thermal contact than the one in which silicone grease was used and minimized the local depression in the surface temperature at the point of measurement (45, p. 394). An even better thermal contact was realized when the adhesive substance was removed from the back of the copper tape and a small amount of strain gage adhesive, M-Bond 200 Adhesive and 200 Catalyst, was applied on two opposite corners of the copper tape. Care was taken that the middle portion of the copper tape remained "clean" and in intimate contact with the surface. This was a



very tedious process, but was nevertheless repeated for every heat sink tested. See a discussion of the errors resulting from using this procedure in Section 3.3.

In an attempt to minimize the thermal resistance between the heater element and the base of the heat sink a thin layer of a zinc oxide loaded silicone grease was applied to the base. The grease used was Dow Corning 340 Thermal Joint Compound, whose thermal conductivity was approximately  $0.00745 \text{ W/(cm)(}^{\circ}\text{C)}$  (43, 46, 47). It was illustrated that the application of DC-340 to mating surfaces could decrease thermal resistance between surfaces by 200% compared to that of a dry joint (48). Following this operation the heater was placed between the pair of heat sinks and the resulting assembly was then clamped in the desired test position. This concluded the preparations involved in the assembly of the heat sinks.

The other part of preparation procedure dealt with getting the equipment ready for data taking. The air conditioning vents in the room were carefully blocked, using paper and duct tape. They were checked every day for possible air leaks. Although small air disturbances were probably present they did not affect the temperature readings of a few thermocouples placed in the air around the test section. Indeed, temperature readings of the surrounding medium were found to be very stable throughout the course of the experiment. The fact that data were taken after the hour at which the air conditioning system was shut down in the whole building contributed even more to the belief that the environment was "appropriate" for a natural convection experiment.

An average of the measurements of two thermocouples placed laterally at about 30 cm distance from the set up provided the value used for  $T_{\infty}$ .

Previous to a run the instruments were turned on and allowed to warm up for about thirty minutes in order to reach equilibrium. The next step was to standardize the K-3 potentiometer and afterwards to use it as a reference to zero-adjust the ammeter and voltmeter. This sequence of standardize-zeroing operation was carried out at least one other time during the course of a run. Following this power input was adjusted until a desired temperature was obtained. After steady-state condition was reached, voltage and current values were recorded.

Opinions differ as to what the criterion for determining the attainment of the steady state condition is. Some authors (38) recommend that the same measurement be taken every fifteen minutes for an hour and when subsequent values are identical, steady-state condition is achieved. Others (1) assume the system stabilized if the fluctuations of the test temperature are smaller than  $1^{\circ}\text{C}$  during a ten minute period of time. This writer considered a steady-state condition to be attained if during the last ten minutes of the time interval between two measurements the surface temperature varied by less than  $0.016^{\circ}\text{C}$ . The time allowed between two measurements was approximately thirty minutes.

Between fifteen and twenty power and temperature readings were taken for each run. The range of the temperature difference between the heat sink surface and ambient was from as low as  $0.08^{\circ}\text{C}$  to approximately  $58^{\circ}\text{C}$ . Thermocouples for measuring surface temperatures

were attached to the side of the base, on the base near the pin base and on the tip of the middle pin. A sketch with the locations of thermocouple attachment is shown in Figure III.6.

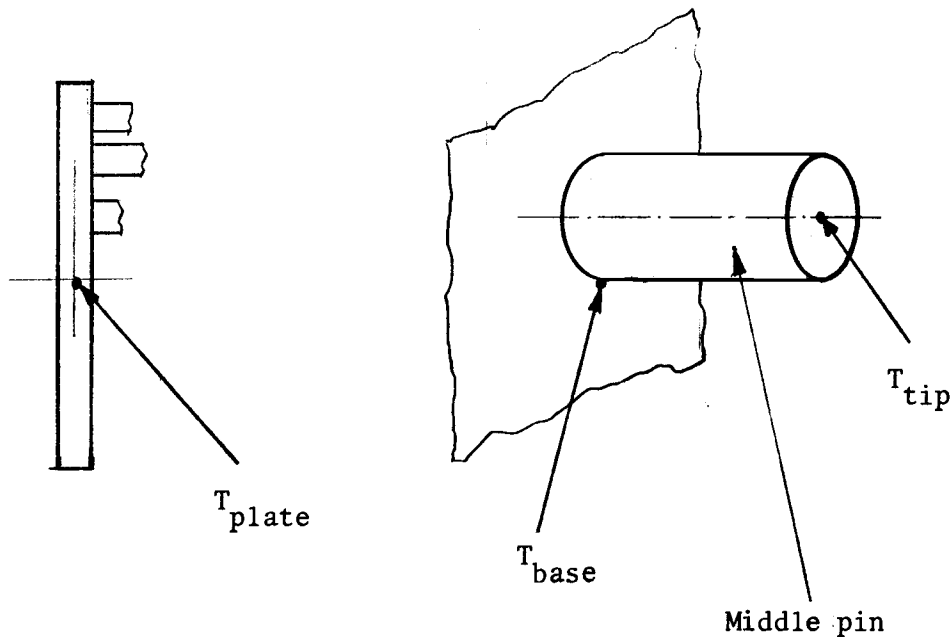


Figure III.6. Sketch with Locations of Thermocouple Attachments

Prior to data taking a test was run to see the variation of the temperature across the plate in a vertical direction. The differences between the temperatures of the lower edge and upper edge of the side and the face of the plate was less than 1.3% in both cases. This showed that the temperature taken at the center of the plate represented a good average value and also that the temperature measured on the base near the fin would be very close to the interior base temperature since the difference between the temperature of the pin base and the side at middle point never exceeded 1.8%. For the last two

or three measurements in each run, fluctuations in the temperature of the tip,  $T_{\text{tip}}^4$  and of the plate side  $T_{\text{plate}}$  were encountered. Several extreme values were recorded for a minute before an arithmetic average was taken. In all cases these fluctuations never exceeded  $\pm 1.3^\circ\text{C}$  or  $\pm 1.1\%$ ; they signaled the beginning of a possible transient flow regime.

Measurements of the heat sink surface temperature were accompanied by temperature measurements of the steel clamps on the clamping device. They were taken at a distance of about 0.5 cm from the end of the clamp which had a 0.038 cm layer of rubber silicone applied in order to insulate it from the plate surface. A discussion of the heat losses through the clamps is given in Section 3.3.

### 3.3. Sources of Errors and Uncertainty Analysis

In presenting the equipment in Section 3.1.3., individual errors associated with the respective pieces of apparatus were presented. It is the intent of this section to present a more detailed discussion of all the errors involved in the experiment and to analyze the uncertainties resulting from the functional correlation between the pertinent parameters and dimensionless groups used in this work.

Errors can be classified according to their origin in four basic types: instrument, computation, human and application errors. They may be systematic (biased), random, or predictable (49). Instrumental errors are due mainly to rounding-off operations and amplification of relative errors resulting from mathematical manipulation of data.

---

<sup>4</sup>Please refer to nomenclature or Figure III.6.

Human errors can result from faulty observations (parallax) or biased readings which appear to be completely random in nature. It is reasonable to believe that the above mentioned sources provide errors that can be neglected in this experiment. Some of the errors are random errors and they obey the laws of probability. The others are systematic in nature and they were minimized by good planning and a repetition of readings, runs, calibration, standardization and zero-setting procedures. Errors belonging to the fourth basic type, application errors, will be discussed next. As mentioned in an earlier section, every effort was made to ensure that any possible source of air disturbances was minimized or eliminated. A good indication that air disturbances were kept to a minimum is that ambient temperature was very stable throughout the experiment.

One possible source of error stemmed from the assumption that power losses through the small gap between the two back-to-back heat sinks were negligible. This assumption is reasonable if one compares the magnitude of the thermal resistance of the heater to the convective thermal resistance at the interface between heater and air. Another potential source of error in evaluating the heat flux is the heat loss from the base of the heat sink to the support through the steel clamps. A comparison between the magnitudes of the thermal resistances and areas involved is shown in Appendix A. It is shown that for the worst case (small heat transfer coefficient and extended surface area) the errors resulting from heat loss through the supports are small.

A possible error could be introduced by the fact that different

temperatures were not measured simultaneously. This error is considered negligibly small due to the stability of the system. Another source of error was the variation of the temperature across the plate. This was treated in Section 3.2., with the variation found to be low, under 2%.

The quality of thermal contact plays an important role in heat transfer between adjacent surfaces. Poor thermal contact increases thermal contact resistance significantly, making the entire device operate inefficiently. In Section 3.2 it was shown how small pieces of copper tape were used in conjunction with the thermocouples for measuring surface temperatures. To answer questions concerning errors in temperature measurement, several runs were made for the same heat sink. It was found that the results agreed within 3.3%. It was therefore concluded that adequate thermal contact existed between the copper tape and the heat sink surface.

Errors in measurements of the plate surface temperature resulting from heat being dissipated away from it along the thermocouple wires by conduction and convection were found to be negligible. Based on an analysis of an arrangement in which a thermocouple is attached to a surface (45), its leads making a 90 degree angle with the surface, the error made in the measurement is given by the formula:

$$T_s - T_t = (T_s - T_\infty) / (1 + 1/B)$$

$$\text{where } B = \pi \left( \frac{k_a k_t}{40 k_s^2} \right)^{1/2} \text{ and subscripts a, t, and s refer to}$$

ambient, thermocouple and surface respectively.

Assumptions made in deriving this relation were that the heat sink was similar to a semi-infinite body at a uniform temperature  $T_s$ , and that the thermocouple wire was an infinitely long, straight, thin fin. The heat transfer coefficient was predicted from an experimental relation for wires, assuming the product  $Gr_D Pr$  to be smaller than  $10^{-5}$ . With this analysis the thermocouple reading was calculated to be less than  $0.5^\circ\text{C}$  below the true value of the surface temperature. This represents a small relative error (0.29%). For the thermocouple attachment method used in this work an even smaller error should be expected since the copper tape provided a larger area at the surface of the heat sink from which heat was withdrawn, producing a smaller depression in the surface temperature. It is interesting to note that the error is independent of the diameter of the wire.

Before discussing the potential sources of errors related to the construction of the heat sinks it should be mentioned here that a small variation of temperature existed along the length of the pins. The maximum temperature difference between the base and tip of a pin was measured to be 6.3%, all others being under 5%. Typically this error was about 3%. This problem will be discussed in more detail in Chapter 4, Heat Transfer Results.

The manner in which the pin fins were attached to the heat sink plate (press fit) allowed the possibility of errors due to poor contact between the pins and the interior surface of the holes drilled in the plate. This possibility was supported by the fact that some of the pins were able to be black anodized only after contact was augmented by peening numerous small holes at the interface between

pins and base. It is important to note that none of the heat sinks to which thermocouples were attached had this problem. The magnitude of the possible error made can be estimated if one assumes the worst case, that is, no contact pressure between the surfaces in question. Using the information given in Figure A2 from the appendix for aluminum surfaces with a surface finish of  $1.65 \times 10^{-4}$  cm (65 $\mu$  in.) thermal resistance per unit area would be about  $0.062^\circ\text{C}/(\text{Watt})(\text{cm}^2)$ , or for the smallest pin (smallest diameter pins were the only affected ones), thermal resistance would be  $0.013^\circ\text{C}/\text{Watt}$ . This is about equal to the thermal resistance of the heat sink found to be  $0.011^\circ\text{C}/\text{Watt}$  and much smaller than the convective thermal resistance of the heat sink (about 700 times). To increase confidence in this result, a heat sink was stripped of its black anodized coating to obtain a comparison between data obtained before and after the contact between the pins and the base was improved. After the stripping process the diameters of the pins became slightly smaller (0.091 cm compared to 0.0941 cm). The emissivity of the surface was also different since the stripping process was a chemical one compared to the mechanical process utilized initially. Nonetheless, a comparison between data was made and the agreement was good; the largest difference found<sup>5</sup> was 5.16%.

Flatness of the mounting surfaces is the most important factor in ensuring a low thermal resistance. Special attention is given by heat sink manufacturers to the tolerances describing the flatness of the surfaces involved in mechanical contact. The range of deviation

---

<sup>5</sup>In fact the largest error found was 22.2% and the next largest was 5.16%. It is believed that a faulty recording or reading provoked this large error.



from extreme to extreme of a surface flatness is expressed as cm/cm total indicator runout (TIR). Heat sinks typically are built having a TIR between 0.005 cm/cm and 0.013 cm/cm. The measured average flatness of the back plate of the heat sink was about 0.004 cm/cm. A potentially critical factor was the flatness of the heater. However, due to the softness of the heater insulation and to the relative large clamping pressure, this problem was minimized. Moreover, the thin layer of 340 Dow Corning Heat Sink Compound improved thermal contact by minimizing the adverse effects of possible high TIR and poor surface finish.

The last source considered is one related to the functional relationship existing between certain variables. A brief discussion of the functional uncertainty concept is given in Appendix B. According to this, the uncertainty involved in evaluating the heat flux was 0.38%.

#### IV. THERMAL DESIGN AND HEAT TRANSFER RESULTS

##### 4.1. Thermal Design

The designer is frequently in need of means for comparing the thermal performance of different heat sinks. Tables and graphs yielding these design parameters are of practical use in this case. In this section comparisons of the performances of the heat sinks studied in this work will be given, along with procedures that will enable the designer to select a suitable heat sink for a given application.

As stated earlier, the use of heat sinks is necessary when the temperature of an electronic component must be kept below a certain value. This is the reason why one of the parameters used in the first set of graphs is the temperature rise of the base of the heat sink above that of the ambient. This will be the maximum temperature difference; it is plotted against the power dissipated by the heat sink in Figures IV.1 through IV.4. The data presented in each plot are for a constant pin diameter and a specified surface finish. Six different sets of points are shown for each of the three different pitch-to-diameter ratios and two pin arrangements (rectangular and triangular). Figures IV.1, IV.2 and IV.3 show the results for the heat sinks having a black anodized surface, while Figure IV.4 is for the case of a polished surface finish and smallest pin diameter only. In all cases, with the exception of the smallest pin diameter, those heat sinks with black anodized surfaces had superior performances compared to those with bright polished surfaces.

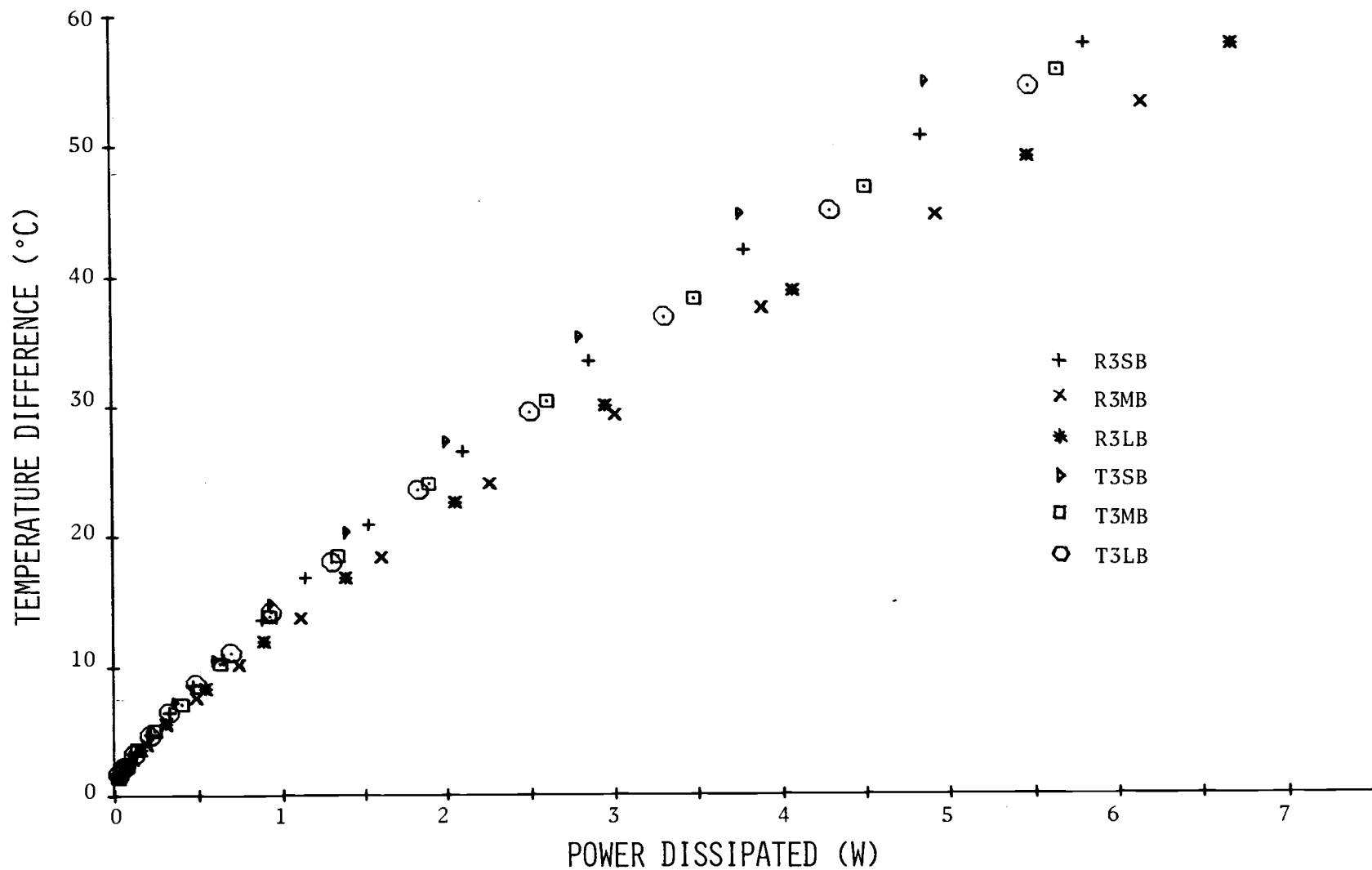


Figure IV.1. Variation of Temperature Difference with Power Dissipated for  $D = 0.238$  cm and a Black Anodized Surface

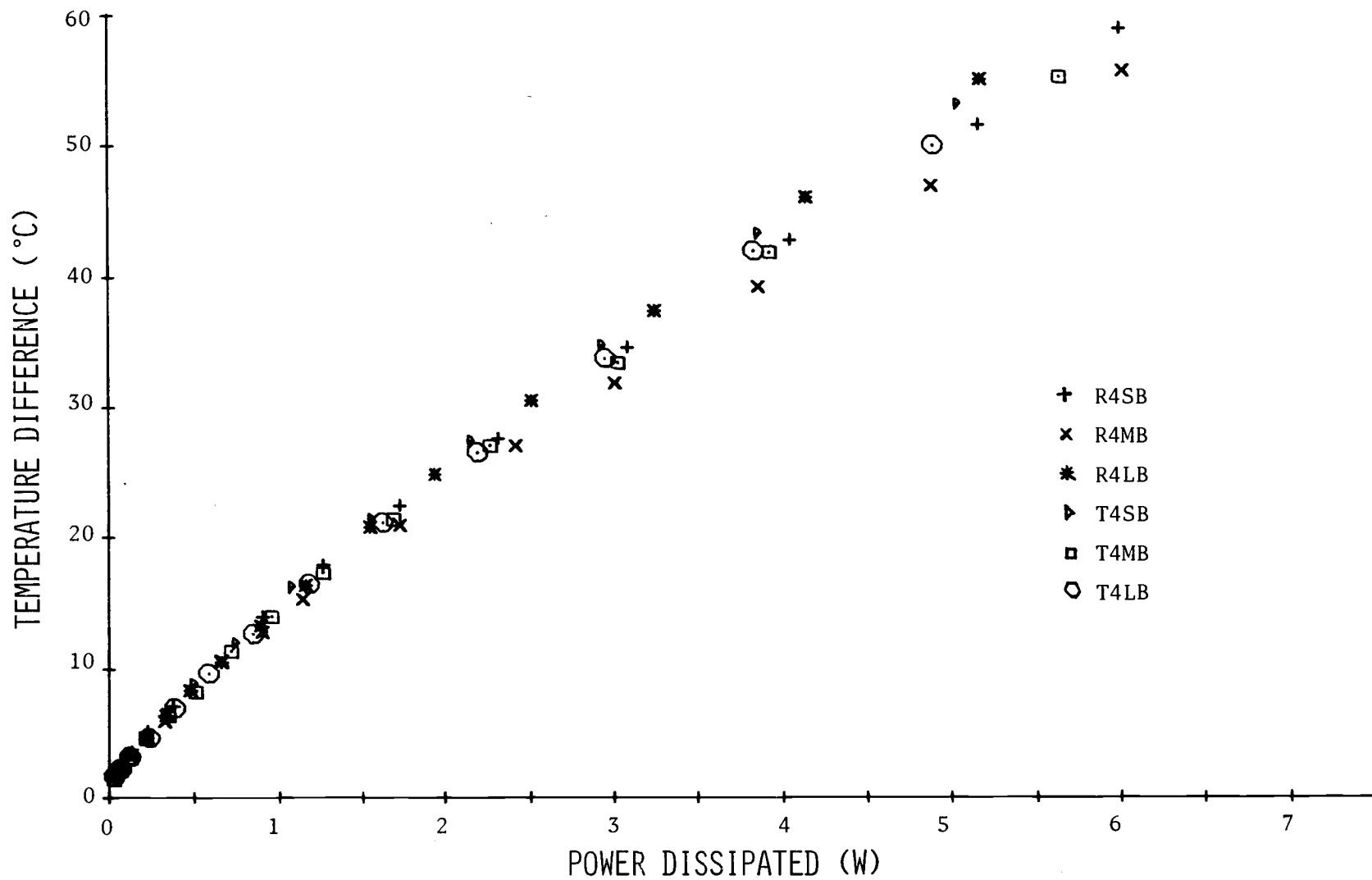


Figure IV.2. Variation of Temperature Difference with Power Dissipated for  $D = 0.318$  cm and a Black Anodized Surface

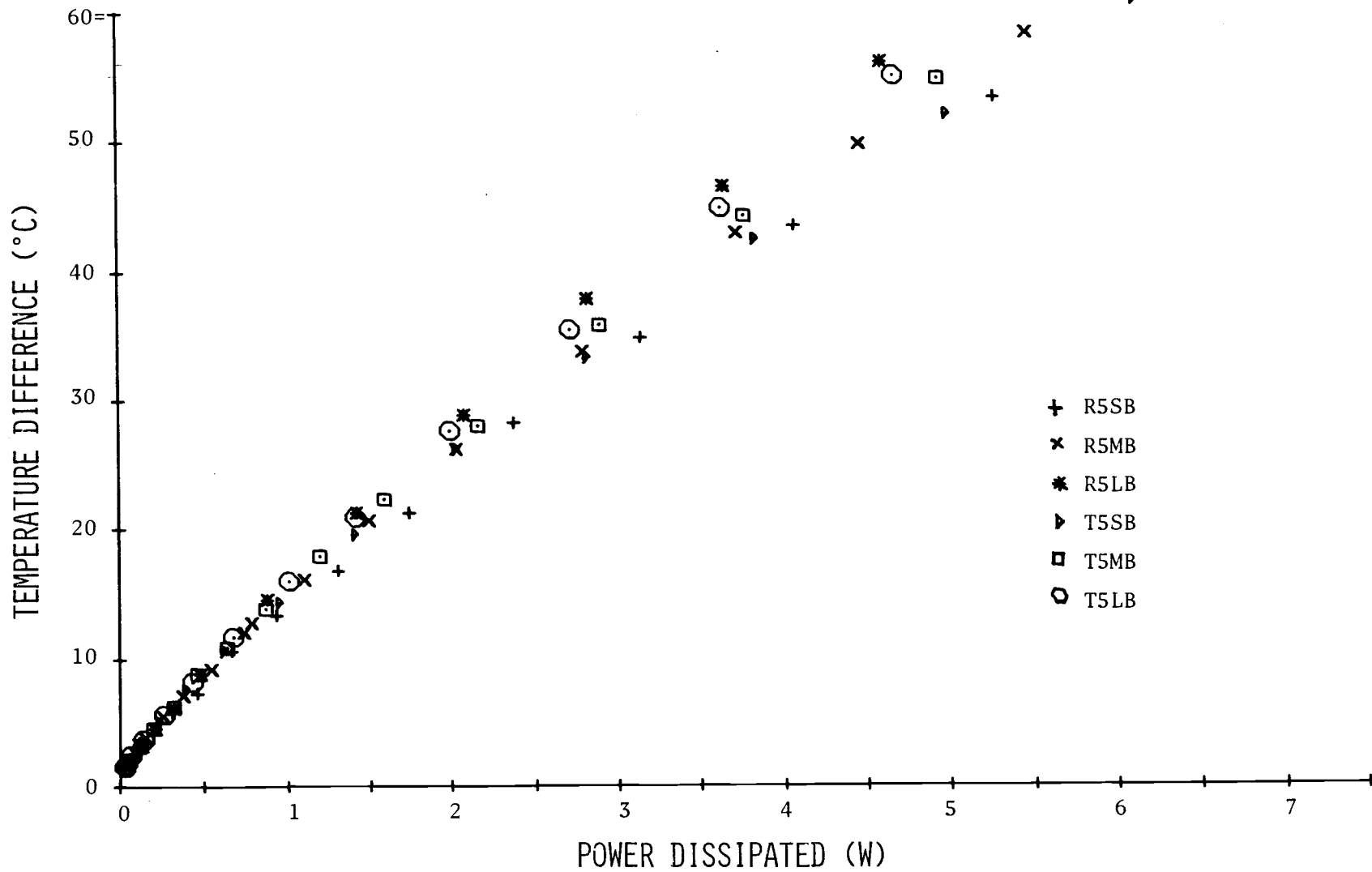


Figure IV.3. Variation of Temperature Difference with Power Dissipated for  $D = 0.396$  cm and a Black Anodized Surface

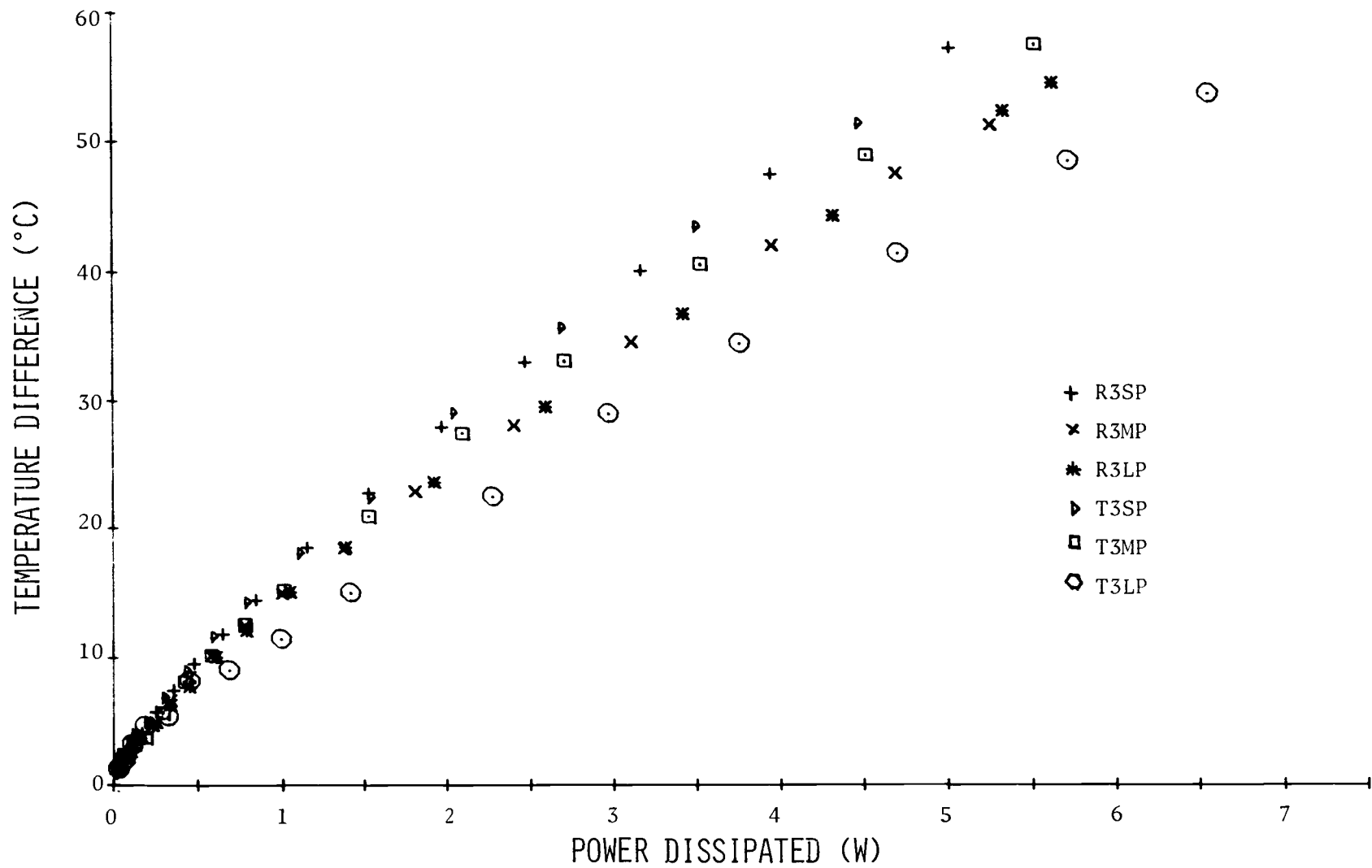
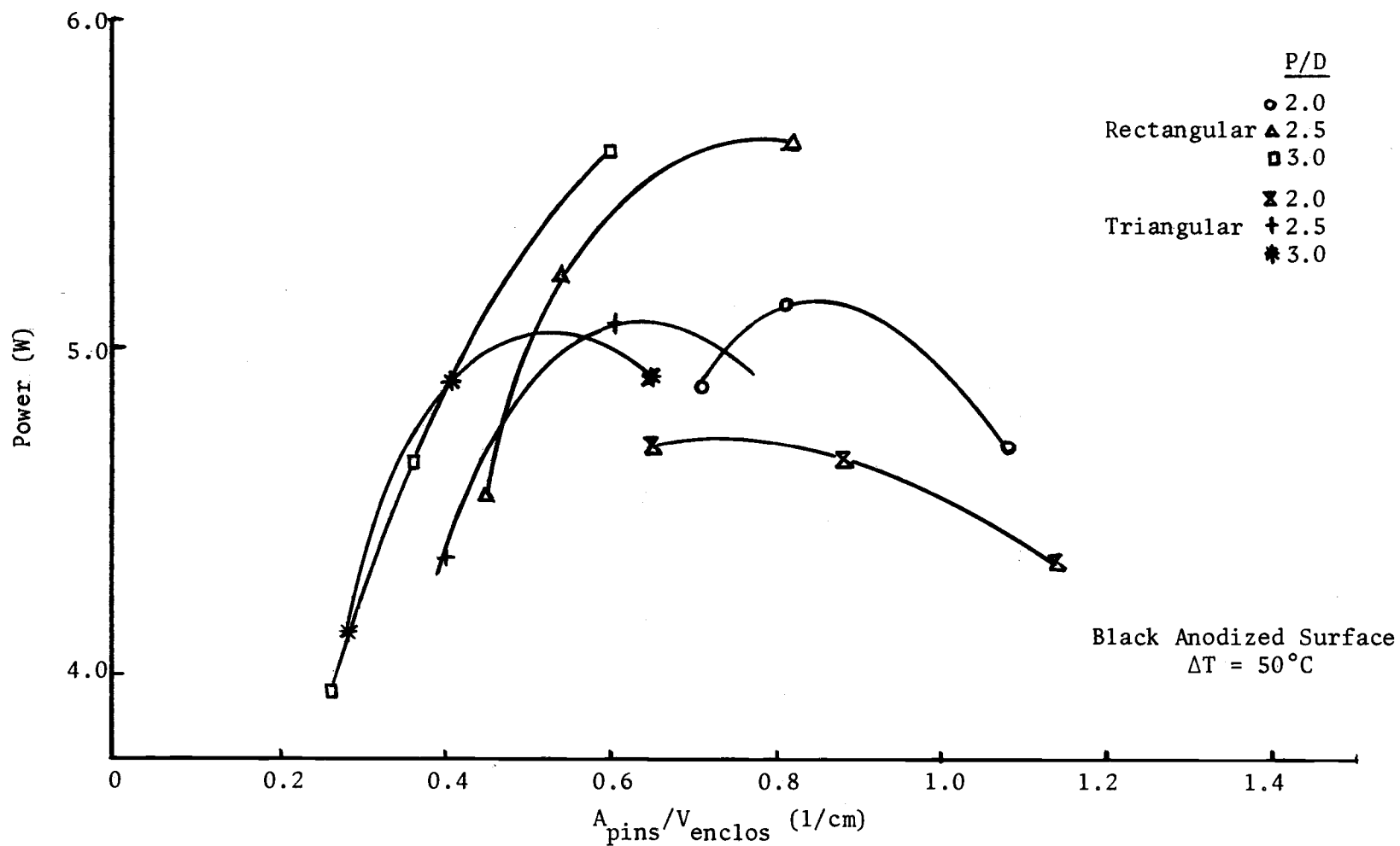


Figure IV.4. Variation of Temperature Difference with Power Dissipated for  $D = 0.238$  cm and a Polished Surface

The performance of the heat sinks is affected by the result of the interaction between the effects of four parameters: diameter, spacing, pin arrangement and surface finish. For heat sinks with the smallest diameter pins, those having medium and large spacing dissipated approximately the same power for a given temperature difference. The poorer heat transfer performance for the closest spacing and small diameter is due to the interference of the developing boundary layers of two neighboring pins. For the medium diameter (0.318 cm), rectangular pattern heat sinks, the poorest heat dissipating characteristics are exhibited by the largest spacing and the best heat dissipating characteristics by the medium spacing (see Figure IV.2). For the largest pin diameter examined (0.397 cm) in a rectangular pattern (Figure IV.3), the smallest pitch-to-diameter ratio gives the best characteristics and the largest pitch-to-diameter ratio gives the worst. T3LP heat sink (Figure IV.4) performs better than T3LB; this could **not** be explained satisfactorily since the only difference between them is the surface finish. A test could not be run to check this geometry.

Figure IV.5 presents the variation of the dissipated power as a function of the ratio between the total surface area of the pins and the volume of an enclosure formed by a cube having the length of a side equal to the side of the base of the heat sink. It is clear that rectangular pin arrangements are better than triangular ones for black anodized heat sinks if powers larger than 5W are to be dissipated. This is a surprising result. In fact it appears that a heat sink with pins in triangular arrangement would not be able to dissipate more than 5W and maintain a temperature difference of 50°C. Heat sinks with pins in



IV.5. The Variation of the Power Dissipated with the Area-Volume Ratio for Black Anodized Surfaces



rectangular arrangements and with large spacing would dissipate around 15% more power. If the values of the power dissipated are between 4 and 5W, indications are that a heat sink with triangular pin arrangement with a spacing of  $P/D = 3$  has effectively the same behavior as one with a rectangular pin arrangement and the same spacing. Black anodized heat sinks with rectangular pin arrangements and large spacings present the best overall characteristics.

A procedure for designing an appropriate heat sink can be outlined easily. For a desired power dissipation several alternatives are available. Knowing how much space is available, the surface area of the pins for the highest power dissipation can be found. Diameter of the pin can then be determined. The designer must choose between power dissipation characteristics and cost of fabrication.

The results presented in Figure IV.5 were evaluated using the three values of  $P/D$  ratios for which data were obtained. The shapes of the curves drawn through these data show consistent behavior.

#### 4.2. Heat Transfer Results

The results obtained in the previous section were presented in a form that pertains to a specific application, that of heat sinks used as cooling devices. In order to obtain more general results and to be able to analyze the variation of heat transfer characteristics in respect to the parameters involved in this study, a different presentation of data is necessary.

It is interesting to examine the variation in "effective" thermal resistance of the heat sinks plotted as a function of pitch-

to-diameter ratio. This is illustrated in Figures IV.6 and IV.7. The heat transfer coefficient involved in the effective thermal resistance includes radiation effects; the area used is the contact area of the heat sink. The interest in these results stems from the designer's need of knowing the total thermal resistance along the heat transfer path between the electronic component and the surroundings. This way the power that must be dissipated from an electronic device in order to keep its temperature at a certain value can be found. The lower the effective thermal resistance of the heat sink, the higher the value of the power dissipation for a given temperature difference. It is important to remember that the lowest thermal resistance of a heat sink does not necessarily correspond to the maximum heat transfer coefficient, that is, the values of  $P/D$  for which the heat transfer coefficient and the heat transfer rate are maximum might not be the same [see Pan and Knudsen (36)].

From Figure IV.6 and IV.7 one may observe the maximum difference between the heat sink with the lowest thermal resistance (for a diameter of 0.238 cm, black anodized) and the one with the highest to be  $3.8^{\circ}\text{C}/\text{W}$ . The difference between the lowest thermal resistances for the rectangular and triangular arrangements is about  $0.5^{\circ}\text{C}/\text{W}$  while the difference between the black anodized and polished heat sinks with small diameters and triangular arrangement is about  $1.2^{\circ}\text{C}/\text{W}$ . It is important to note that these values were obtained for a temperature difference of  $50^{\circ}\text{C}$ .

Another observation from Figures IV.6 and IV.7 is that the black anodized heat sinks with rectangular pin arrangement demonstrate

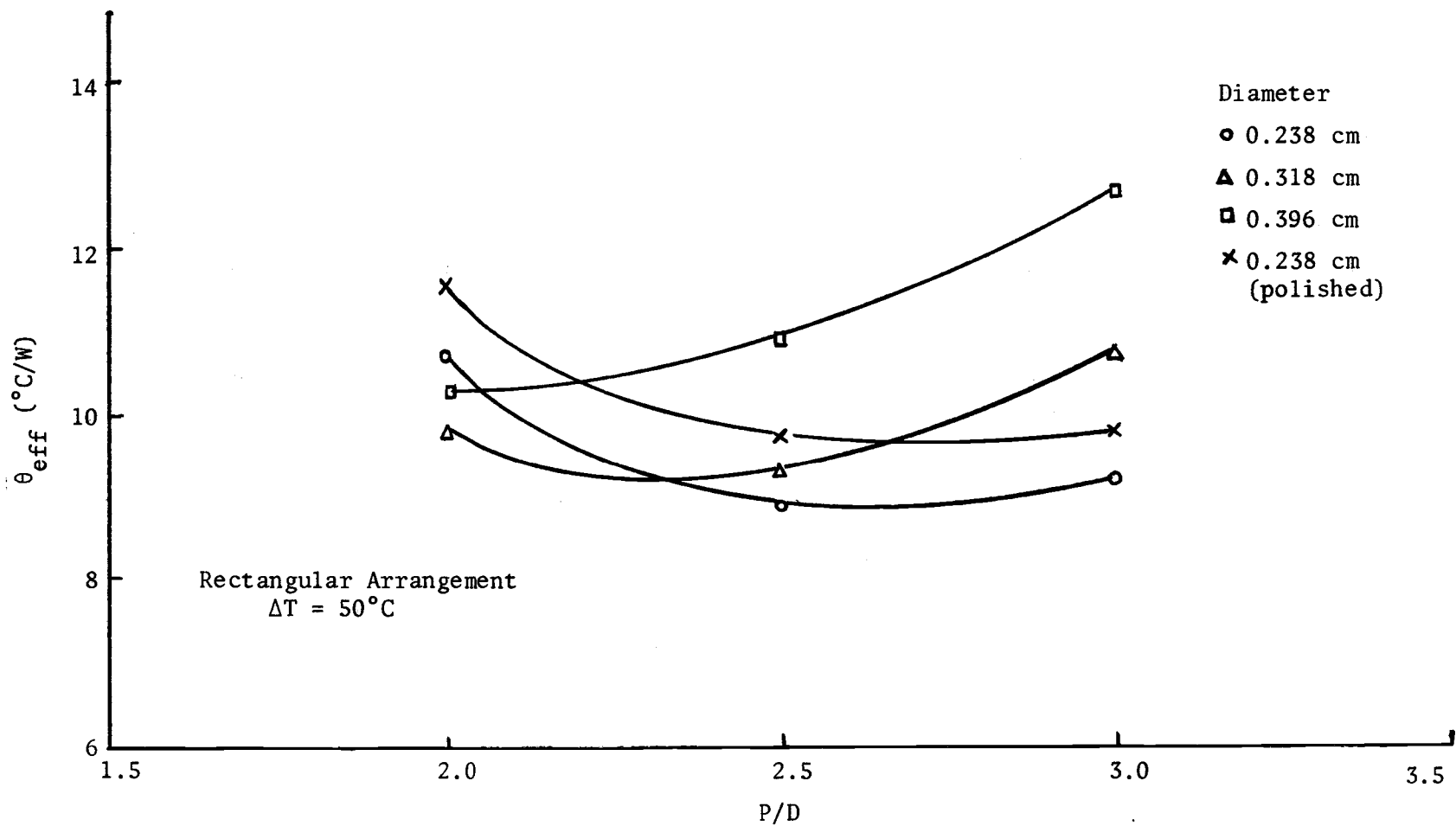


Figure IV.6. The Variation of the Effective Thermal Resistance with P/D for Rectangular Arrangement

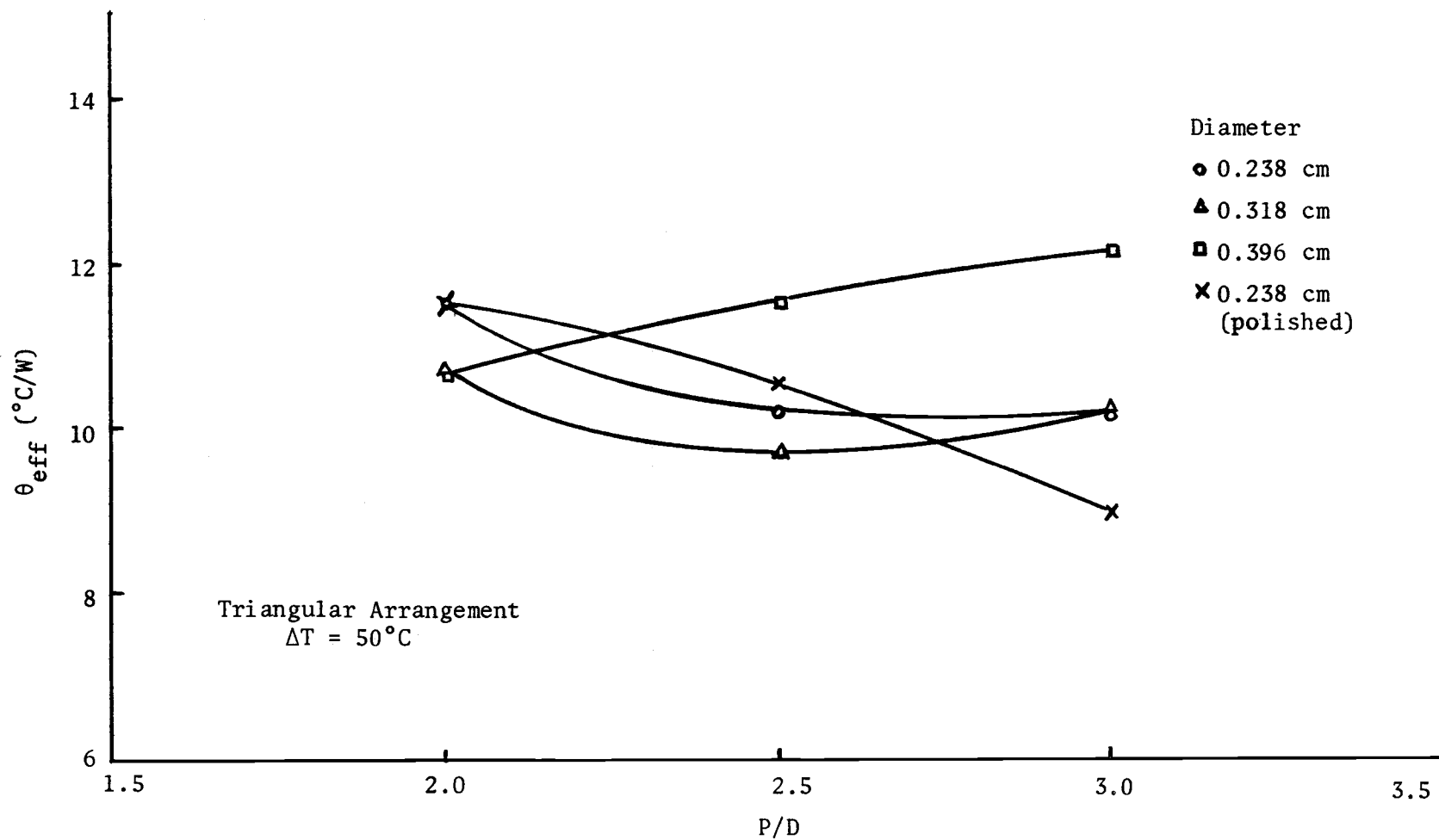


Figure IV.7. The Variation of the Effective Thermal Resistance with P/D for Triangular Arrangement

superior performances compared with those having a triangular arrangement over a range of  $P/D$  between 2.0 and 2.8. Outside this range of variation of  $\theta_{eff}$  cannot be predicted from available data. The apparent irregular manner in which thermal resistance varies with  $P/D$  for the two pin arrangements can be explained by the influence of the surface area of the pins upon the product  $hA$ . Due to the way the heat sinks were made, some of these triangular pin arrangements had fewer pins than did those with rectangular patterns, even though  $D$  and  $P/D$  were the same; this in turn means a smaller surface area and thus a higher effective thermal resistance. A better comparison of the pin arrangements would be obtained if the thermal resistance would be based on an equal area which would mean, in fact, the variation of the inverse of the heat transfer coefficient with  $P/D$ . Such variation was not plotted.

Another explanation for the superiority of the rectangular pin arrangement over the triangular one for the black anodized heat sinks is that in the triangular pattern radiation reduces the heat transfer capabilities due to the increased view factor between a pin and its neighbors and the corresponding decreased view factor between a pin and its surroundings. Therefore, less energy can be exchanged between the pins and the surrounding surfaces by radiation when the surfaces are black, compared to when they are polished. This idea is also supported by the fact that for the polished finish the triangular pin arrangement proves to be a better one.

The heat transfer coefficient provides relationships among several variables, such as surface temperature, ambient temperature, fluid

properties, surface area and heat transfer rate, which are the fundamental variables encountered in natural convection. It would therefore be most useful to obtain results that correlate all these. The obvious way to represent these variables is to arrange them in dimensionless groups that arise naturally from the dimensional analysis of the governing momentum and energy equations. These are the Nusselt, Grashof and Prandtl numbers. The meaning and development of these dimensionless groups were discussed in Section 2.1. Since the medium is air and the temperature differences encountered are relatively small, Prandtl number will have a small variation and thus will contribute little in the relationship between the dimensionless groups mentioned above. Therefore, the log of Nusselt number is plotted against the log of Grashof number. The raw data were reduced to Grashof and Nusselt number form, using the computer program NUGR listed in Appendix D. The plotting was done using a routine developed at Oregon State University called EZPLOT.

It was difficult to determine what characteristic length should be used with the Nusselt and Grashof numbers. It was decided that the results could be better used if a simple dimension (either length, pitch or diameter) would be implied. The chosen dimension was pin diameter since Grashof number based on pitch can easily be obtained from the one based on the diameter. The Grashof number based on length would not be representative for this work in which length was a constant.

In the evaluation of  $Nu_D$  and  $Gr_D$ , the acceleration of gravity,  $g$ , was taken as constant:

$$g = 980.6 \text{ cm/sec}^2$$

The temperature dependence of the other properties was accounted for by evaluating these properties at a reference temperature,  $T_{\text{ref}}$ , using the following expressions:

$$\beta = 1/T_{\infty} (^{\circ}\text{C})^{-1}$$

$$\rho = P/RT_{\text{ref}} = 71.4135/T_{\text{ref}} \quad \left(\frac{\text{gm}}{\text{cm}^3}\right)$$

$$c_p = 0.219 + 0.342 \times 10^{-4} T_{\text{ref}} - 0.293 \times 10^{-8} T_{\text{ref}}^2 \quad (\text{Btu/lbm-}^{\circ}\text{R})$$

$$\mu = (145.8 \times 10^{-7} T_{\text{ref}}^{3/2}) / (110.4 + T_{\text{ref}}) \quad \left(\frac{\text{gm}}{\text{cm-sec}}\right)$$

$$k = (0.6325 \times 10^{-5} T_{\text{ref}}^{1/2}) / (1 + 245.4/T_{\text{ref}} \times 10^{-12}/T) \quad (\text{cal/cm-sec-}^{\circ}\text{K})$$

All expressions are given in their original forms in the references. The expression for specific heat was taken from a paper by Spencer and Justice (50), viscosity was obtained from a Sutherland-type formula and it was taken from the NBS-NACA Tables (51), while the expression for the thermal conductivity was taken from a paper by Glassman and Bonilla (52).

Sparrow and Gregg (53) recommended that for a tube bundle the reference temperature for evaluating fluid properties should be taken as the arithmetic average between the temperature of the heat sink

surface and that of the surroundings;  $T_{ref} = 0.5T_s + 0.5T_\infty$ . Choosing a representative surface temperature of the heat sink was not a problem in this study since rather small temperature variations existed along the base and pins of the heat sinks. In Sections 3.2 and 3.3 it was shown that between the base and tip of the pins the largest temperature difference found was 6.3%, with a typical value of 3%, while between the side of the plate and base of the pins this variation was only 1.8%. An arithmetic average was taken between the base and tip temperature of the pin. If the material used would have been one of lower thermal conductivity a weighted average of the temperature of the side, pin and base would have been employed. This average would have been based on the area of the pins and plate and on a given temperature profile along the pins. This technique was developed but it is not presented in this work.

Due to the number of geometrical parameters used in this study, the task of determining these effects upon the process of convection from the heat sinks was not an easy one. Spacing, for example, affects the heat transfer in several ways. For a close spacing surface area is relatively large and the heat transfer coefficient small, with other variables kept constant. The hydrodynamic boundary layers of adjacent pins interfere, decreasing the heat transfer coefficient. On the other hand for small spacings the so-called "chimney" effect is obtained, which consists of confinement of the air in small spaces which results in greater buoyant forces thus a higher  $h$ . Finally, for a small  $P/D$  ratio the radiative view factor from a pin to the surrounding pins increases complicating analysis of the radiant contribution



to total heat transfer. This process becomes even more complicated if one considers the simultaneous influence of pin diameter, arrangement and surface finish.

Figures IV.8 through IV.13 show the influence of spacing upon the heat sinks with triangular and rectangular pin arrangements and black surface finish. For each set of plots diameter was constant. Data presented in the first three diagrams, Figures IV.8, IV.9 and IV.10, were obtained by a rectangular pin arrangement, black anodized surface and for three diameters in all three figures. Data for the larger spacing,  $P/D = 3.0$ , show a higher Nusselt number than for medium and small pitch-to-diameter ratios. For the closest spacing it is apparent that the interference of the momentum boundary layers of the horizontally-adjacent pins constituted the predominant effect. An expected fact that can be observed from the same figures is that  $Nu_D$  increases with the increase in the pin diameter.

Similar patterns are exhibited by data shown in Figures IV.11, IV.12 and IV.13 for triangular pin arrangement. The larger spacing displays again the highest Nusselt numbers. A comparison of  $Nu_D$ - $Gr_D$  data for different diameters shows again the larger pin diameter yielding higher  $Nu_D$ . Unlike the cases of rectangular pin arrangement, data for the triangular pin arrangement display anomalous behavior for large and medium  $P/D$  at values of Grashof number between about 3 and 10 for all pin diameters. With this triangular arrangement in the low  $Gr_D$  range there is indication that the data may approach a single asymptote or that the lines may intersect. The lack of precision in this range and small amount of data make a definitive conclusion

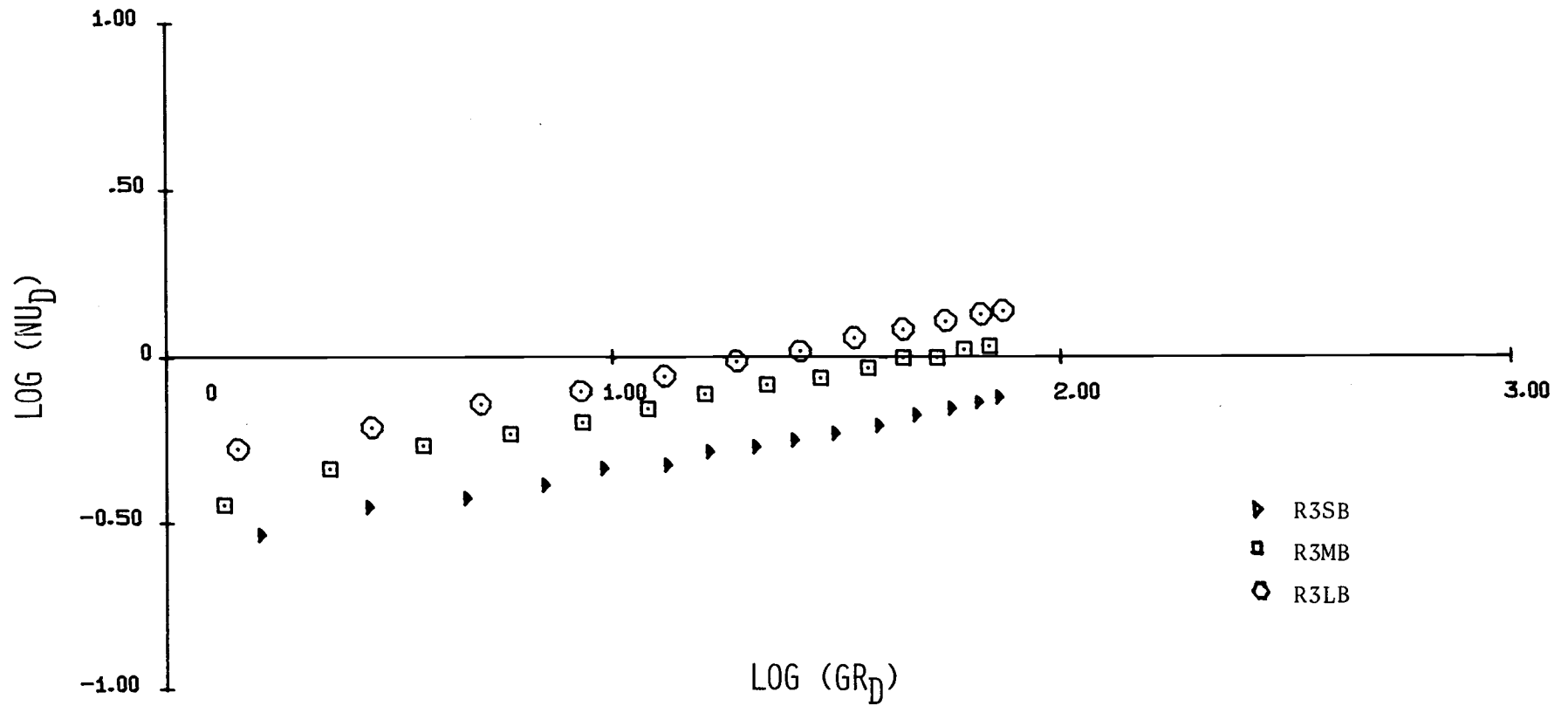


Figure IV.8. Average Heat Transfer Results for  $D = 0.238$  cm, Rectangular Pin Arrangement, Black Anodized Surface and  $P/D = 2.0, 2.5$  and  $3.0$

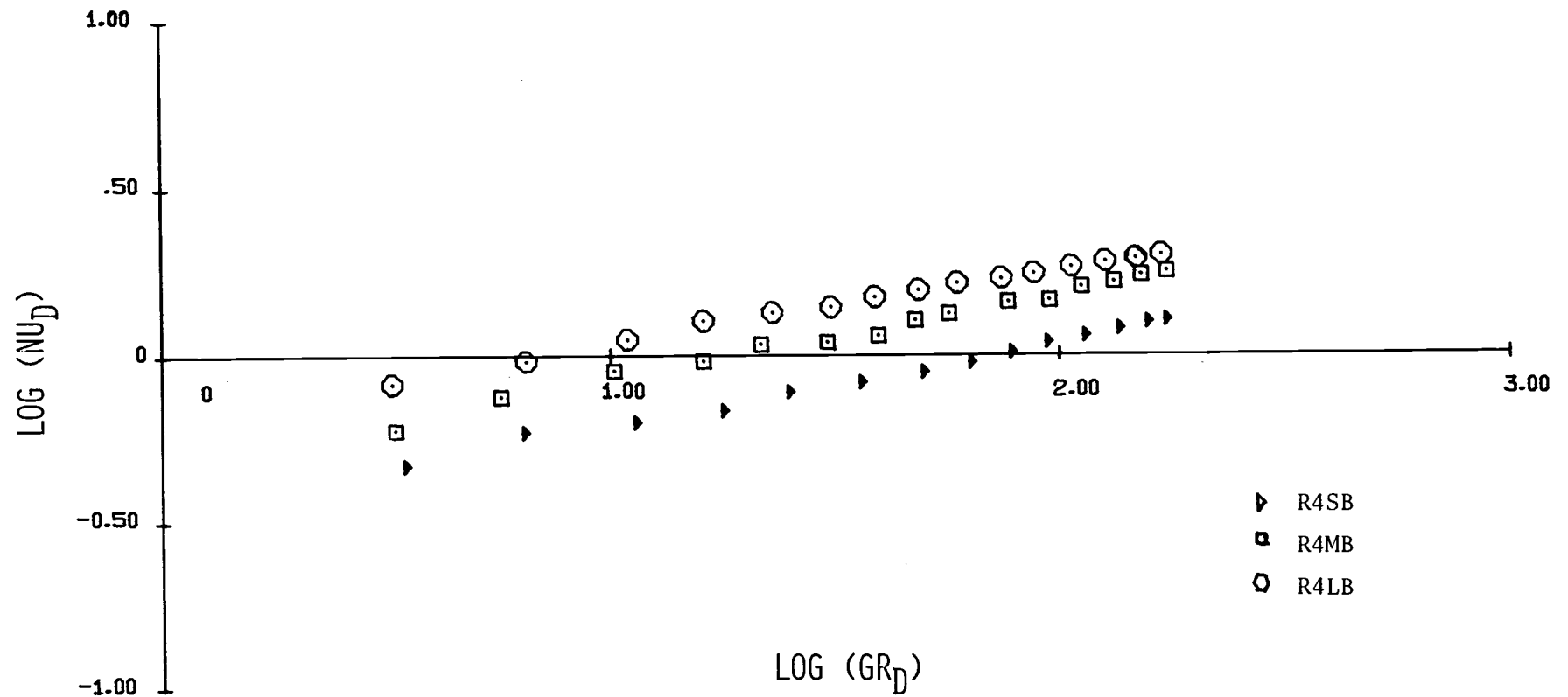


Figure IV.9. Average Heat Transfer Results for  $D = 0.318$  cm, Rectangular Pin Arrangement, Black Anodized Surface and  $P/D = 2.0, 2.5$  and  $3.0$

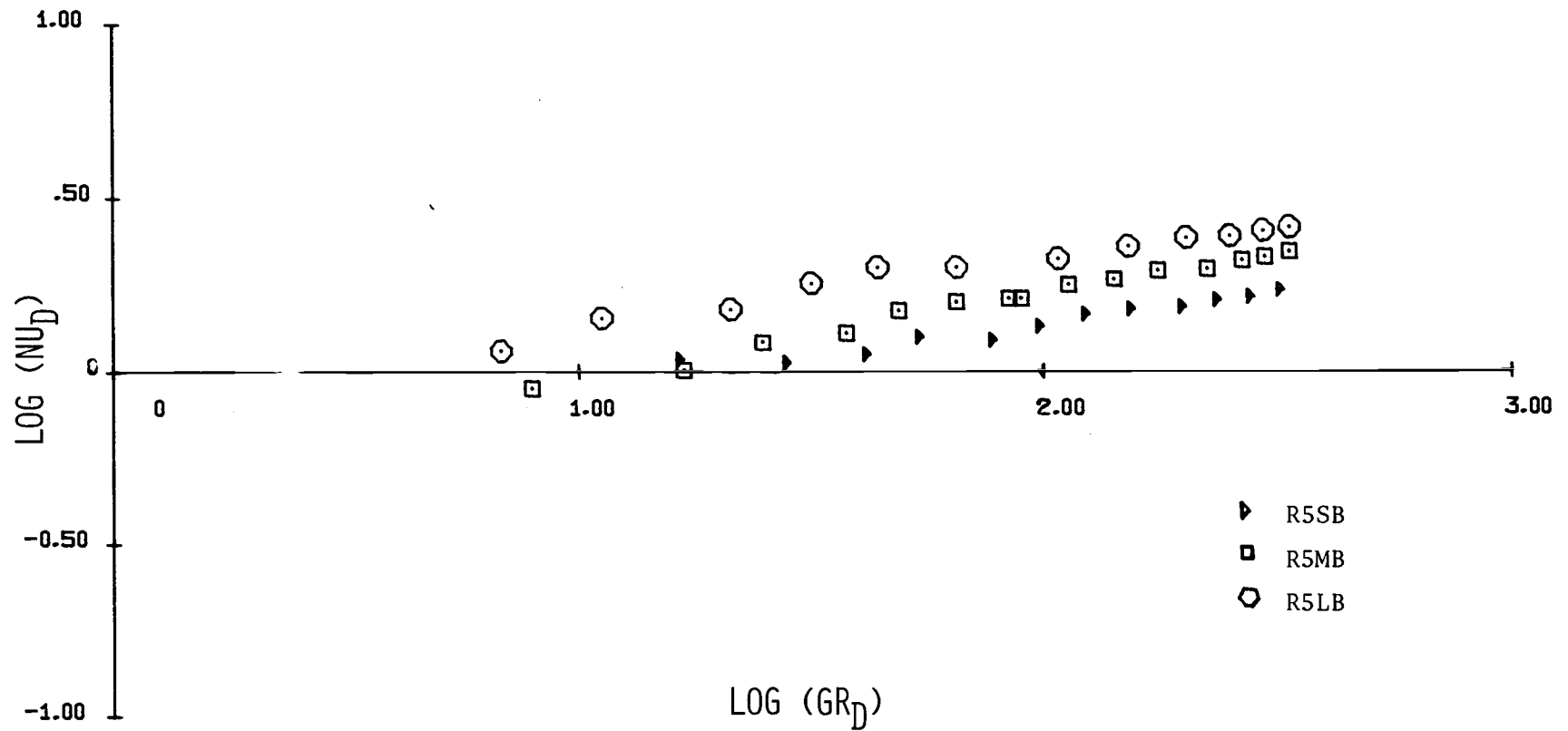


Figure IV.10. Average Heat Transfer Results for  $D = 0.396$  cm, Rectangular Pin Arrangement, Black Anodized Surface and  $P/D = 2.0, 2.5$  and  $3.0$

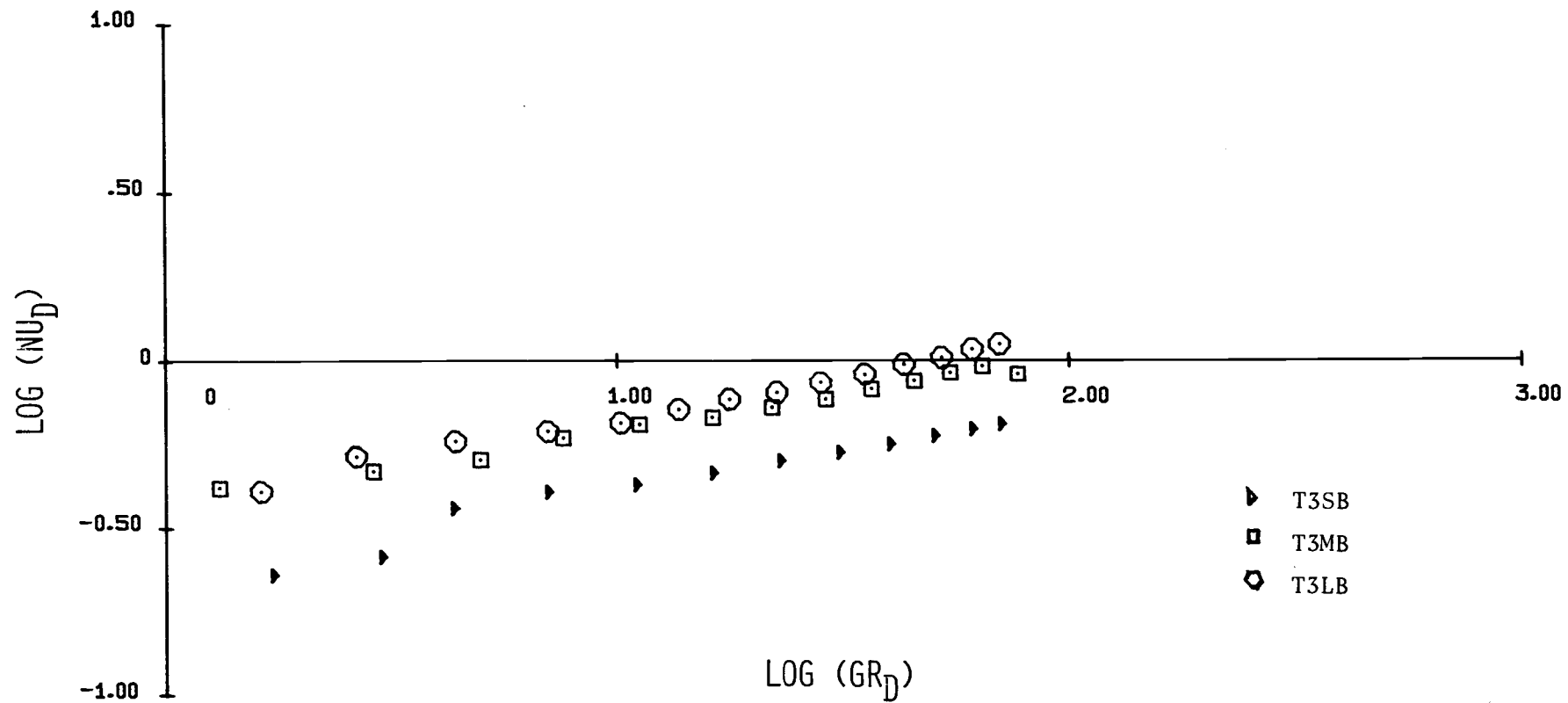


Figure IV.11. Average Heat Transfer Results for  $D = 0.238$  cm, Triangular Pin Arrangement, Black Anodized Surface and  $P/D = 2.0, 2.5$  and  $3.0$

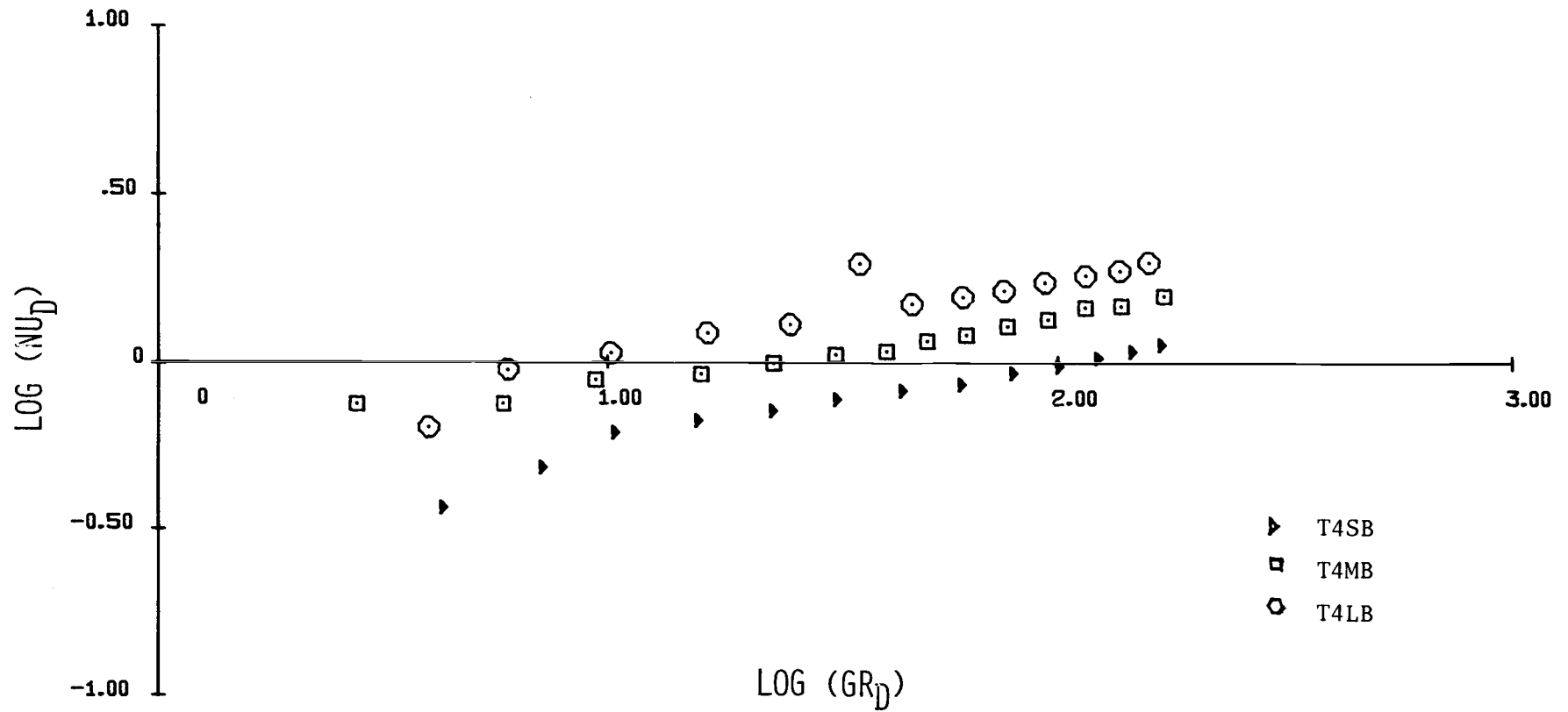


Figure IV.12. Average Heat Transfer Results for  $D = 0.318$  cm, Triangular Pin Arrangement, Black Anodized Surface and  $P/D = 2.0, 2.5$  and  $3.0$

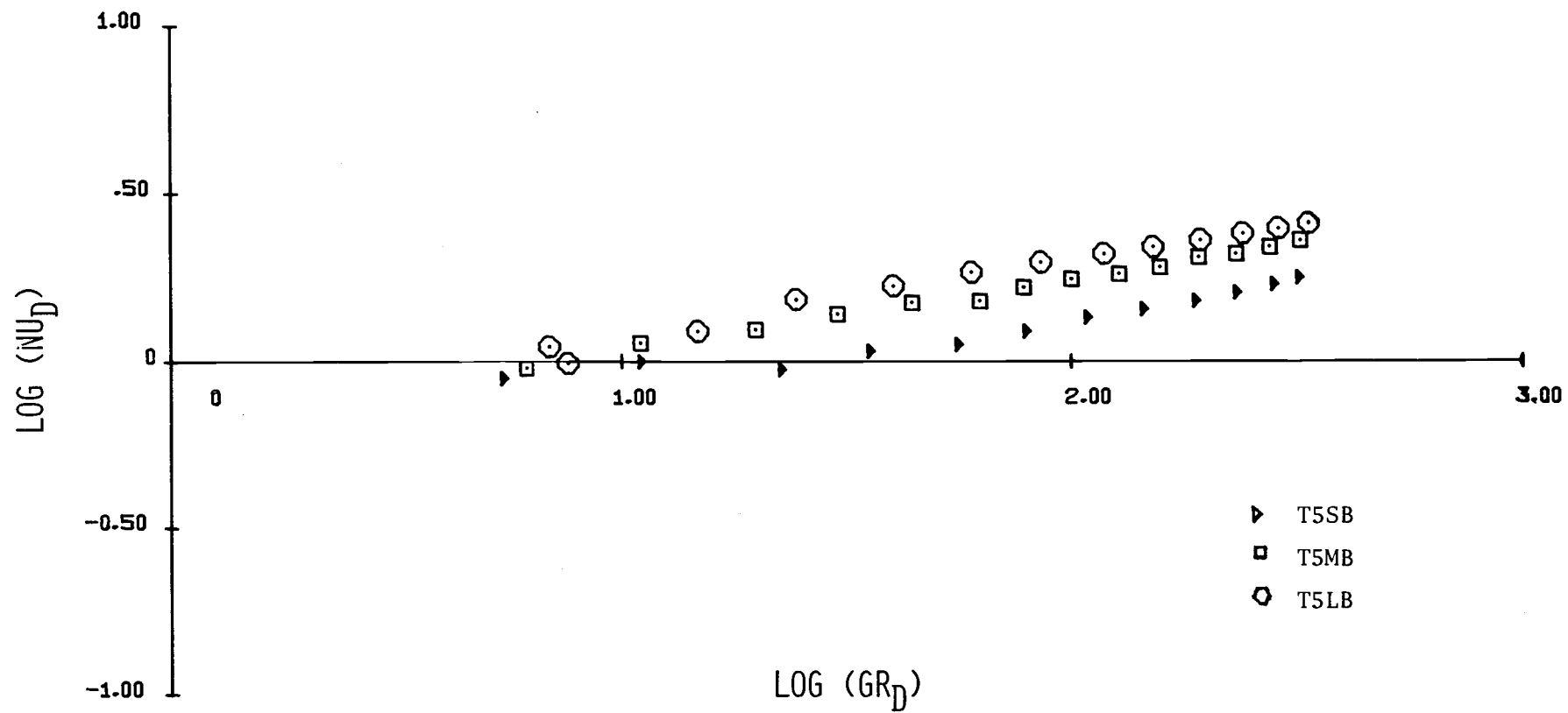


Figure IV.13. Average Heat Transfer Results for  $D = 0.396$  cm, Triangular Pin Arrangement, Black Anodized Surface and  $P/D = 2.0, 2.5$  and  $3.0$

impossible.

Figures IV.14, IV.15 and IV.16 show comparisons between: the data for rectangular and triangular patterns; polished and black surfaces; all spacings and smallest diameter. It appears that for  $Gr_D$  greater than 10, the rectangular pin arrangement with black surface finish presents the highest  $Nu_D$  for every spacing. For the same range of  $Gr_D$  of all spacings the largest P/D offers the highest heat transfer coefficient. For values of Grashof number lower than 10, however, the curves are sufficiently close to one another that it is difficult to determine any trends.

The difficulty in explaining the relationship between  $Nu_D$ - $Gr_D$  at low values of  $Gr_D$  is because in this region the pins behave like small wires. In his experiment Elenbaas (27) finds an implicit relationship between  $Gr_D$  and  $Nu_D$  for values of  $Gr_D$  smaller than  $10^4$ . Rice (22, 23) and Ekert (14) also studied thin wires in air. The range of Grashof numbers studied in their work extends to about 10 on the lower limit. Senftleben (referenced in 25) studied thin wires for Grashof numbers as low as  $10^{-1}$ . Two comments should be made here. The first is that the geometries studied in this work are much more complicated and as a consequence flow characteristics will be harder to study. There are two types of boundary layers interfering, one for the vertical plate and the other for the horizontal cylinders. The result will have a three dimensional characteristic. Secondly, the relationship between  $Gr_D$  and  $Nu_D$  is not a power law one (This fact is confirmed by the studies mentioned above.). That means that the functional uncertainty value obtained for an analysis based on the power law relationship



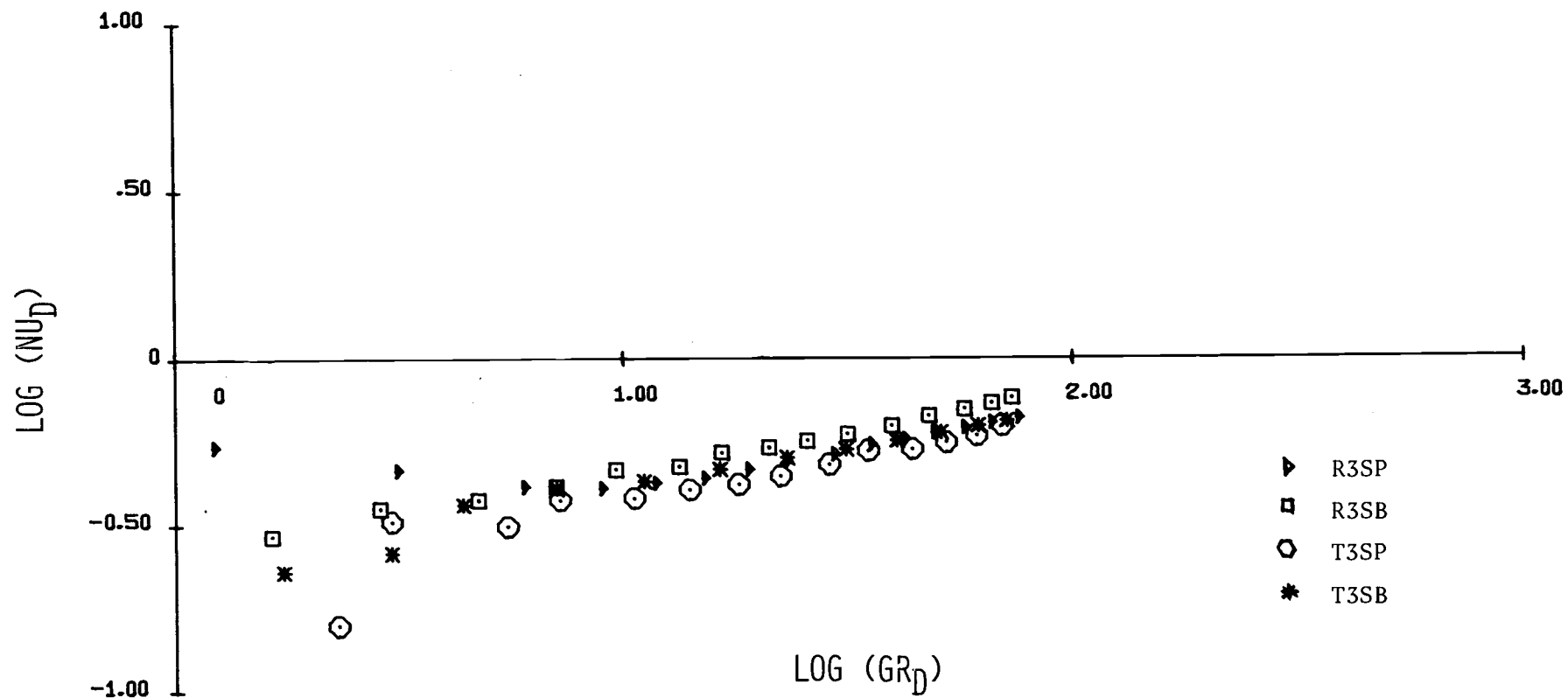


Figure IV.14. Comparison Between Rectangular and Triangular Pin Arrangements, Black and Polished Surfaces, for  $D = 0.238$  cm and  $P/D = 2.0$

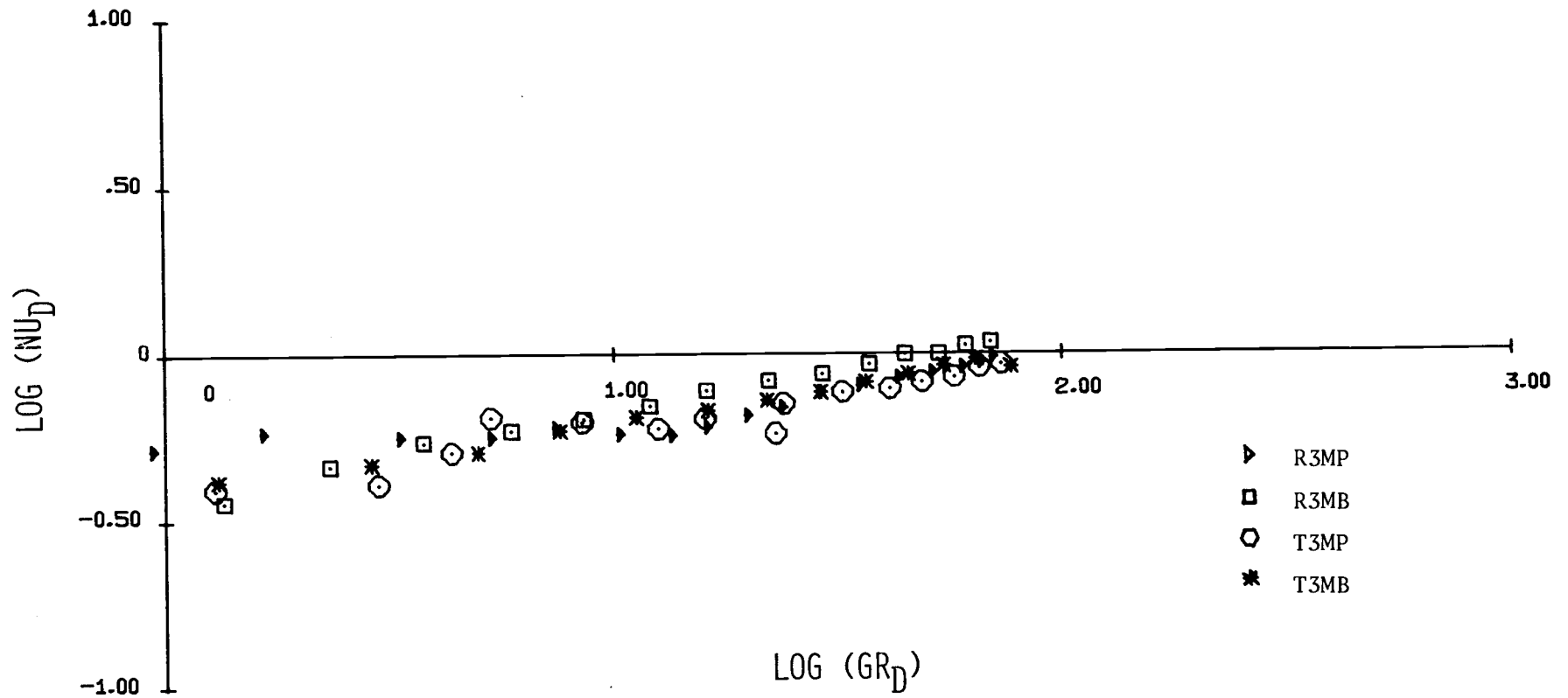


Figure IV.15. Comparison Between Rectangular and Triangular Pin Arrangements, Black and Polished Surfaces, for  $D = 0.238$  cm and  $P/D = 2.5$

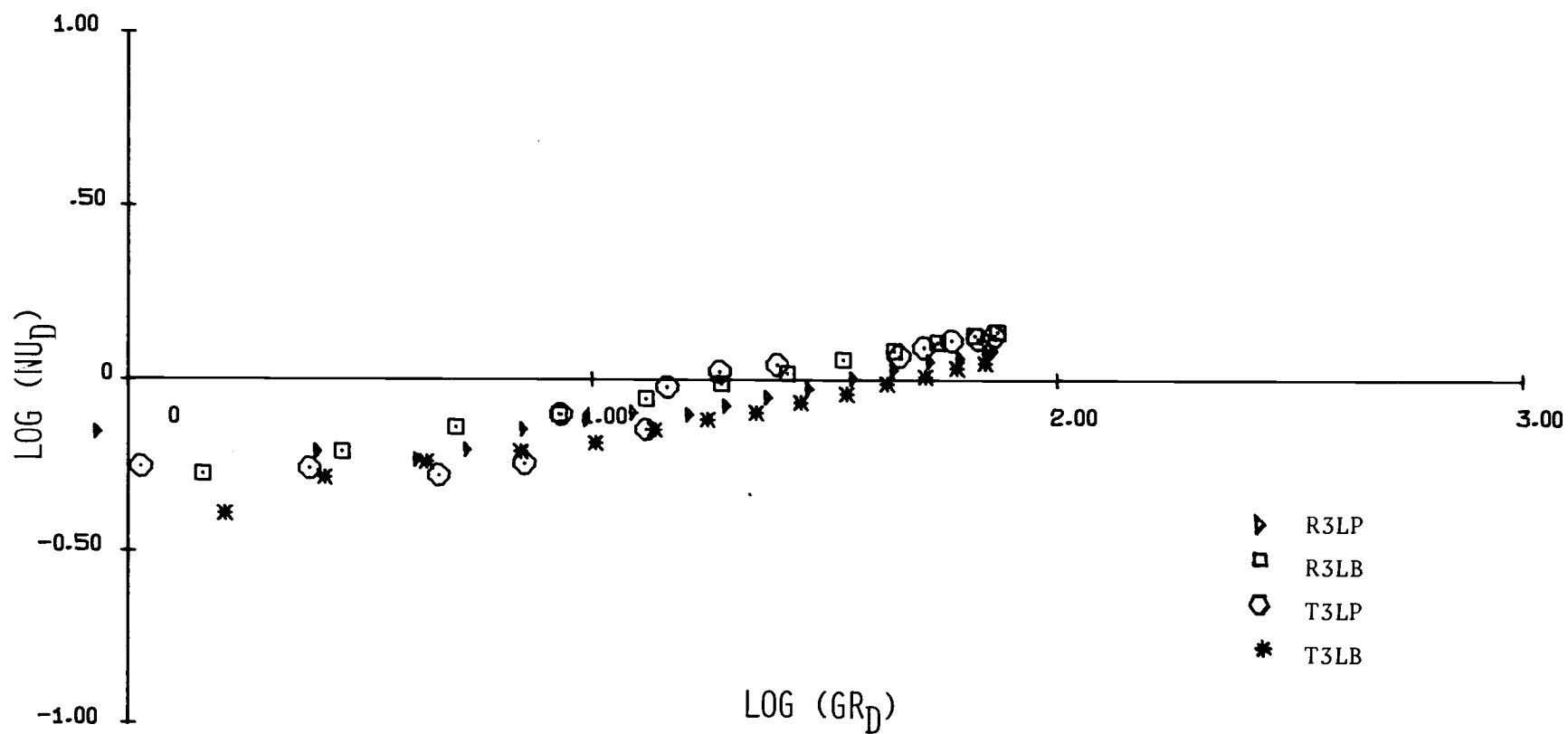


Figure IV.16. Comparison Between Rectangular and Triangular Pin Arrangements, Black and Polished Surfaces, for  $D = 0.238$  cm and  $P/D = 3.0$

between  $Nu_D$  and  $Gr_D$  represents only an estimate.

## V. CONCLUSIONS AND RECOMMENDATIONS

Heat sinks with different pin arrangements, spacings and diameters were studied. Tests were first run for the polished finish and then for the black anodized surfaces. Some important conclusions can now be drawn about the influence of some of the more important parameters upon the power dissipation capabilities and thermal resistance of the heat sinks and about the variation of the heat transfer coefficient.

1. Pin spacing is an important parameter in the heat sink design. It affects the heat transfer rate and it was found that heat sinks with medium and largest pin spacing,  $P/D = 2.5$  and  $3$ , should be employed for good power dissipation characteristics. The pins with  $P/D = 3$  also yielded the highest heat transfer coefficient. The minimum effective thermal resistance was obtained for a  $P/D = 2.5$ . This spacing provides the best combination of heat transfer coefficient and convective area.
2. When a low cost heat sink with high power dissipation characteristics is desired,  $P/D = 3$  represents the pin spacing that should be used.
3. Rectangular pin arrangements present superior heat transfer characteristics over the triangular ones for the black anodized surfaces. A heat sink with a rectangular pin arrangement will also have the minimum effective thermal resistance.
4. Black anodized heat sinks showed better power dissipation characteristics than the polished ones in all cases but one,

a triangular pin arrangement with small diameter, large spacing and polished surface. Because the only difference between T3LP and T3LB is the surface finish, the explanation for this variation must lie in the interaction between convective and radiative heat transfer modes. A satisfactory interpretation of these results could not be found. Due to technological considerations a conclusive test to check the data could not be run for this case.

5. The increase in pin diameter produced an increase in the Nusselt number.
6. A comparison (not shown in this work) was made between heat sink R3LB and typical heat sinks with rectangular fins taken from a current manufacturer's catalog. The pin fin heat sink studied in this work showed 46% and higher power densities ( $\text{W}/\text{cm}^2$ ) at a fixed temperature difference of  $50^\circ\text{C}$ . The heat sinks selected from the catalog had a black anodized surface and were positioned vertically (same as the heat sinks in this study) when tested.

In light of the results of this work and the conclusions drawn from them, a few recommendations can be made:

1. The results obtained for this work should be used only for air and not be extended for other fluids.
2. A study of the velocity profile and the flow patterns is necessary in order to gain insight into the phenomena that take place.

3. The low Grashof number effects upon the heat transfer coefficient should be studied in detail to learn more about the heat transfer in the small wire region.
4. More data should be obtained for other P/D ratios in order to determine the shape of the curves more accurately.
5. It would be of interest to study the effect of the pin length upon the heat transfer characteristics.
6. Additional data for higher temperature differences would be desirable for the designer.
7. A study should be conducted to determine the influence of the inclination of the heat sinks upon the heat transfer characteristics.
8. Finally, the recommendation is made that the heat sinks used in future experiments be casted, even though the cost might be quite high.

## NOMENCLATURE

$A_s, A_b$	surface area and base area of a pin
$A$	area
$B$	$A_b/A$ , for Equation (2.10)
$B$	$\pi \left( \frac{k_a k_t}{40 k_s^2} \right)^{1/2}$ as defined on page 37
$C$	$L^2 P / 3 k A_s$ , notation used by Dusingberre (Equation 2.10)
$c_p$	specific heat
$D$	diameter
$dT$	differential of $T$
$E_b$	total emissive power of a black body
$F(t)$	function used by Cobble
$F_{1-2}$	shape factor for radiation between two bodies
$f(T)$	function of temperature
$g$	acceleration of gravity
$h$	convective heat transfer coefficient
$h'$	effective heat transfer coefficient as used by Dusingberre (Equation 2.10)
$k$	thermal conductivity
$L$	length
$m, n$	exponents
$M, N$	arbitrary coefficients
$P$	perimeter, pitch
$P/D$	pitch-to-diameter ratio



$q$	heat transfer rate
$q'', q/A$	heat flux
$r$	radius
$R$	electrical or thermal resistance
$T_B, T_{base}, T_{ref}$	temperature of the fin base and reference temperature
$T_{tip}, T_{plate}$	temperature of the tip and plate
$T, T_s, T_{surf}$	surface temperature
$T_\infty$	ambient temperature
$t$	thickness
$U(T)$	equivalent function developed by Cobble
$u$	velocity component in x direction (Figure II.1)
$v$	velocity component in y direction (Figure II.1)
$v_\infty$	free stream velocity
$x, y$	axis; x, y direction
$W, \text{Watts}$	units for power

#### Greek Symbols

$\alpha$	thermal diffusivity
$\beta$	coefficient of thermal expansion
$\Delta$	difference
$\delta$	boundary layer thickness
$\epsilon$	emissivity
$\eta$	pin efficiency
$\eta_o$	overall weighted efficiency

$\theta$	thermal resistance
$\lambda$	arbitrary constant
$\mu$	absolute viscosity
$\nu$	kinematic viscosity
$\rho$	density
$\sigma$	Stefan-Boltzmann constant
$\Sigma$	summation
$\Omega_{1-2}$	shape factor for diffuse radiation between two gray bodies
$\omega$	standard deviation, uncertainty

#### Dimensionless Groups

$Gr_D$	average Grashof number based on diameter, $\frac{\beta g D^3 \Delta T}{\nu^2}$
$Nu_D$	average Nusselt number based on diameter, $\frac{hD}{k}$
$Pr$	Prandtl number, $\frac{\nu}{\alpha}$
$Ra_D$	Rayleigh number based on diameter, $Ra_D = Gr_D Pr$

## BIBLIOGRAPHY

1. Spoor, J. Heat Sink Application Handbook, AHAN Inc., Azusa, California (1974).
2. Kraus, A. Cooling of Electronic Equipment, Prentice Hall, Inc., Englewood Cliffs, New Jersey (1965).
3. Drexell, W. H. Convection Cooling, Sperry Engineering Review, 14, n. 1, 25-30 (1961).
4. Elenbaas, W. Dissipation of Heat by Free Convection, Parts I and II, Phillips Research Report, R90 and R95, 3, 338-360, 450-465 (1948).
5. Heiserman, D. L. Heat Pipes for Semiconductor Cooling, Electronics World, 85, n. 6, 37-39 (1971).
6. American Society for Metals. Metals Handbook, Metals Park, Ohio, 1975. (Properties and Selection of Metals, vol. 1).
7. Welty, J. R., C. E. Wicks and R. E. Wilson. Fundamentals of Momentum, Heat and Mass Transfer, John Wiley and Sons, Inc., New York (1969).
8. Hellums, J. D. and S. W. Churchill. Dimensional Analysis and Natural Convection, Chemical Engineering Progress Symposium Series, 57, n. 32, 75-80 (1961).
9. Sparrow, E. M and R. D. Cess. Radiation Heat Transfer, Revised Edition. Brooks/Cole Publishing Co., Belmont, California (1969).
10. Ede, A. J. Advances in Free Convection. In: Advances in Heat Transfer, 4, part I, Academic Press, New York (1967).
11. Schmidt, E. and W. Beckmann. Das Temperatur und Geschwindigkeitsfeld vor einer Warme abgebenden senkrechten Platte bei natuerlicher Konvektion, Tec. Mech. Thermodynam., 1, n. 10, 341-349 (1930).
12. Pohlhausen, E. Das Temperatur und Geschwindigkeitsfeld vor einer Warme abgebenden senkrechten Platte bei natuerlicher Konvektion, Tech. Mech. Thermodynam., 1, 391-406 (1930).
13. Saunders, O. A. Natural Convection in Liquids, Proc. Roy. Soc. (London). Ser. A, 172, n. 948, 55-71 (1939).

14. Eckert, E. R. Introduction to the Transfer of Heat and Mass, McGraw-Hill Book Co., Inc., New York (1950).
15. Ostrach, S. An Analysis of Laminar Free-Convection Flow and Heat Transfer About a Flat Plate Parallel to the Direction of the Generating Body Force, NACA Report 1111 (1953).
16. Sparrow, E. M. Laminar Free Convection on a Vertical Plate with Prescribed Nonuniform Wall Heat Flux or Prescribed Nonuniform Wall Temperature, NACA TN 3508 (1955).
17. Sparrow, E. M. and J. L. Gregg. Laminar Free Convection from a Vertical Plate with Uniform Surface Heat Flux, Trans ASME, 78, 435-440 (1956).
18. Ostrach, S. Laminar Flows with Body Forces. In: High Speed Aerodynamics and Jet Propulsion, 4, Princeton University Press, Princeton, New Jersey (1964).
19. Hermann, R. Heat Transfer by Free Convection from Horizontal Cylinders in Diatomic Gases, NACA Technical Memorandum 1366 (1954), (Translated from German, VDI Forschungshft, 379, 1936).
20. Jodlbauer, K. Das Temperatur und Geschwindigkeitsfeld um ein Gehiztes Rohr Bei Freier Konvektion, Forschung Gebiete Ingenieurw., 4, n. 4, 157-172 (1933).
21. Langmuir, I. Convection and Conduction of Heat in Gases, Physical Review, 34, 401-422 (1912).
22. Rice, C. W. Free Convection of Heat in Gases and Liquids, Trans A.I.E.E., 42, part I, 653-665 (1923).
23. Rice, C. W. Free Convection of Heat in Gases and Liquids, Trans A.I.E.E., 43, part II, 131-144 (1924).
24. King, W. J. The Basic Laws and Data of Heat Transmission, Mech. Engr., 54, 347-350 (1932).
25. McAdams, W. H. Heat Transmission, McGraw-Hill Book Co., New York (1954).
26. Mueller, A. Heat Transfer From Wires to Air, Trans AIChE, 28, 613-629 (1942).
27. Elenbaas, W. The Dissipation of Heat by Free Convection From Vertical and Horizontal Cylinders, J. of Applied Physics, 19, 1148-1154 (1948).

28. Van de Hegge Zijnen, B. G. Modified Correlation Formulae for the Heat Transfers by Natural and by Forced Convection from Horizontal Cylinders, Appl. Sci. Res.(A), 6, 129-140 (1956).
29. Hsu, S. T. Engineering Heat Transmission, Third Edition, McGraw-Hill Book Co., Inc., New York (1954).
30. Sesonske, A. Velocity & Temperature Distributions About a Horizontal Cylinder in Free Convection Heat Transfer, AIChE J., 7, n. 2, 352-353 (1961).
31. Nakai, Seiichi. Heat Transfer From a Horizontal Circular Wire at Small Reynolds and Grashof Numbers, Int. J. Heat Mass Transfer, 18, n. 3, 387-413 (1975).
32. Holman, J. P. Heat Transfer, Second Edition, McGraw-Hill Book Co., Inc., New York (1968).
33. Cobble, M. H. Nonlinear Fin Heat Transfer, University Park, New Mexico, 1963, 21 p. (New Mexico State University Engineering Experiment Station. Technical Report no. 13).
34. Collicott, N. E. and W. E. Fontaine. Free Convection and Radiation Heat Transfer From Cylindrical Fins, Trans ASHRAE, 71, part II, 148-151 (1965).
35. Edwards, J. A. and J. B. Chaddock. An Experimental Investigation of the Radiation and Free-Convection Heat Transfer From a Cylindrical Disk Extended Surface, Trans ASHRAE, 69, 313-322 (1963).
36. Pan, R. B. and J. G. Knudsen. Convection Heat Transfer From Transverse Finned Tubes, Chemical Engineering Progress, 59, no. 7, 45-50 (1963).
37. Dusenberre, G. M. Effective and Local Surface Coefficients in Fin Systems, Trans ASME, 80, 1596-1598 (1958).
38. Starner, K. E. and H. N. McManus, Jr. An Experimental Investigation of Free Convection Heat Transfer From Rectangular Fin Arrays, Trans ASME, J. of Heat Transfer, Ser. C, 85, 273-278 (1963).
39. Welling, J. R. and C. B. Wooldridge. Free Convection From Rectangular Vertical Fins, Trans ASME, J. of Heat Transfer, Ser. C, 87, 439-444 (1965).
40. Harahap, F. and H. N. McManus, Jr. Natural Convection Heat Transfer From Horizontal Rectangular Fin Arrays, Trans ASME, J. of Heat Transfer, Ser. C, 89, 32-38 (1967).

41. Bergles, A. E. and R. I. Webb. Bibliography on Augmentation of Convective Heat and Mass Transfer, ASME Winter Annual Meeting, New York (1970).
42. Baker, H. D., E. A. Ryder and N. H. Baker. Temperature Measurement in Engineering, John Wiley and Sons, Inc., New York (1953).
43. Scott, A. W. Cooling of Electronic Equipment, John Wiley and Sons, Inc., New York (1974).
44. Gubareff, G. G., J. E. Janssen and R. H. Torborg. Thermal Radiation Properties Survey. Second Edition. Honeywell Research Center, Minneapolis, Minnesota (1960).
45. Chapman, A. J. Heat Transfer, The MacMillan Company, New York (1960).
46. Thermalloy Inc. Heat Sinks for Semiconductor Devices, Catalog No. 73-HS-9, Dallas, Texas (1973).
47. Wakefield Engineering Inc. Wakefield Semiconductor Heat Sinks, Catalog No. 103A, Wakefield, Massachusetts (1976).
48. Bergles, A. E., R. C. Chu and J. H. Seely. Survey of Heat Transfer Techniques Applied to Electronic Equipment, ASME Winter Annual Meeting, New York (1972).
49. Tuve, G. L and L. C. Domholdt. Engineering Experimentation, McGraw Hill Book Co., Inc., New York (1966).
50. Spencer, H. M. and J. L. Justice. Thermal Properties of Gases, Journal of American Chemical Society, 56, p. 2311 (1934).
51. NBS-NACA Tables of Thermal Properties of Gases, U. S. Department of Commerce, National Bureau of Standards, compiled by R. L. Nuttall et al. (1950).
52. Glassman, I. and C. F. Bonilla. Thermal Conductivity and Prandtl Number of Air at High Temperatures, Chemical Engineering Progress Symposium Series, 49, n. 5, 153-161 (1953).
53. Sparrow, E. M. and J. L. Gregg. The Variable Fluid--Property Problem in Free Convection, Trans ASME, 80, 879-886 (1958).
54. Lieberman, J. and B. Gebhart. Interactions in Natural Convection from an Array of Heated Elements, Experimental, International Journal of Heat & Mass Transfer, 12, 1385-1396 (1969).

## APPENDICES

## APPENDIX A

Analysis of the Thermal Circuit of the Heat Sink Assembly

The system analyzed below is composed of: heat sink, clamps plus insulation and support. The equivalent electric circuit is given in Figure A.1.

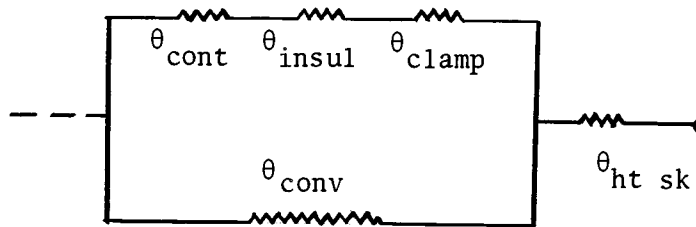


Figure A.1. Equivalent Thermal Circuit of the Heat Sink Assembly

The overall thermal resistance of this circuit is given as:

$$\theta = \theta_{ht\ sk} + \theta_{equiv} \text{ where } \theta_{equiv} = \frac{1}{1/\theta^* + 1/\theta_{conv}}$$

$$\text{where } \theta^* = \theta_{cont} + \theta_{insul} + \theta_{clamp}$$

The symbols  $\theta_{cont}$ ,  $\theta_{insul}$ , and  $\theta_{clamp}$  represent the equivalent thermal resistances for eight contacts, insulation layers and clamps respectively. They were obtained by:

$$\theta_{cont} = (1/8)(\theta_{i\ cont})$$

$$\theta_{insul} = (1/8)(\theta_{i\ insul})$$

$$\theta_{clamp} = (1/8)(\theta_{i\ clamp})$$



1. Thermal contact resistance between the silicone rubber insulating layer and heat sink surface will be approximated by using Figure A.2, which was taken from Scott (43). The worst case will be assumed, that is, a minimum contact resistance in order to maximize the loss of heat. For this case, aluminum on aluminum data will be used, realizing that for a softer material like silicone rubber thermal resistance will be even lower. Assume:

--50 psi clamping pressure

--aluminum on aluminum

--25.4 $\mu$ cm surface finish

From Figure A.2 get  $\theta_{i \text{ cont}}/A_{\text{cont}} = 0.019^\circ\text{C}/(\text{W})(\text{cm})^2$

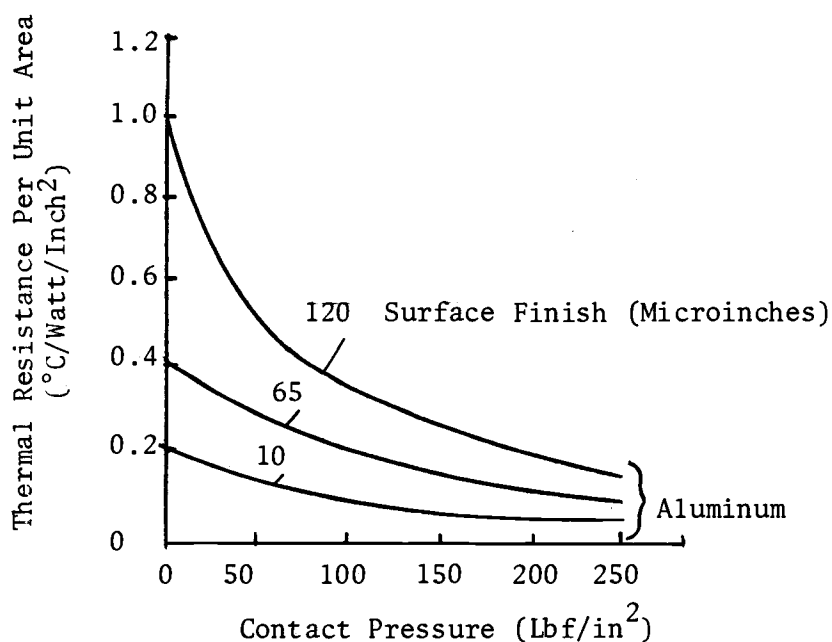


Figure A.2. Thermal Resistance of Interfaces as a Function of Contact Pressure

$$A_{\text{cont}} = 0.016 \text{ cm}^2$$

$$\theta_{i \text{ cont}} = 3.04 \times 10^{-4} \text{ }^{\circ}\text{C/W}$$

$$\theta_{\text{cont}} = 3.7 \times 10^{-5} \text{ }^{\circ}\text{C/W. This last value is negligible.}$$

2. A clamp and the support can be modeled as shown in Figure A.3.  
The sketch is not to scale and all dimensions are given in centimeters.

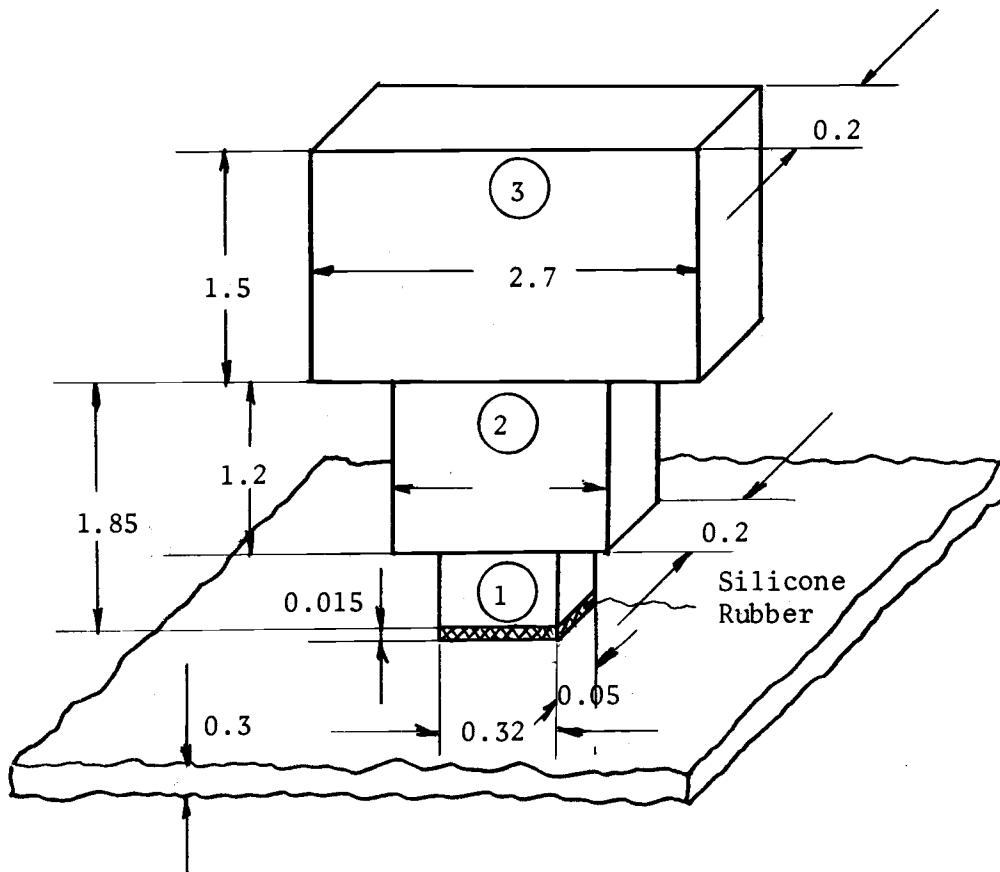


Figure A.3. Model Representing the Clamp and the Support

The equivalent thermal resistance of the clamp and part of the support is:

$$\theta_{i \text{ cl}} = \theta_1 + \theta_2 + \theta_3 = \frac{L_1}{k_s A_1} + \frac{L_2}{k_s A_2} + \frac{L_3}{k_s A_3} = \frac{1}{k_s} \left[ \frac{L_1}{A_1} + \frac{L_2}{A_2} + \frac{L_3}{A_3} \right]$$

The material is stainless steel with a thermal conductivity of 0.16 W/(cm)(°C).

$$L_1 = 0.65 \text{ cm}; L_2 = 1.2 \text{ cm}; L_3 = 1.5 \text{ cm}$$

$$A_1 = 0.016 \text{ cm}^2; A_2 = 0.12 \text{ cm}^2; A_3 = 0.54 \text{ cm}^2$$

The total resistance of the clamp is:<sup>6</sup>

$$\theta_{i \text{ cl}} \approx 334^\circ\text{C/W}$$

$$\theta_{\text{tot clamp}} = (1/8)(334) \approx 42^\circ\text{C/W}$$

3. Thermal resistance of the insulating silicone rubber is now considered. The thermal conductivity of silicone rubber, according to Scott (43), is:

$$k = 1.97 \text{ W/(cm)(}^\circ\text{C)} \times 10^{-3}$$

Measured thickness of layer,  $t = 0.0381 \text{ cm}$

$$\theta_{i \text{ insul}} = \frac{t}{kA} \approx 1,209^\circ\text{C/W}$$

$$\theta_{\text{insul}} = 151^\circ\text{C/W}$$

---

<sup>6</sup>This resistance will be in reality higher since the clamp is in direct thermal contact with the body of the support which has a relatively small cross-sectional area.

4. The convective thermal resistance is maximum when the heat transfer coefficient is minimum.<sup>7</sup> In this case  $h \approx 1.136 \times 10^{-3} \text{ W/}(\text{cm})^2(\text{°C})$  and area is minimum (least number of fins, biggest diameter). Total convective area is:

$$A_{\text{conv}} = 22.71 + 25.094 \approx 48 \text{ cm}^2$$

$$\theta_{\text{conv}} = \frac{1}{hA_{\text{conv}}} = 18.3 \text{ °C/W}$$

Comparing the thermal resistance of insulation and clamp with the convective one ( $\theta = 193 \text{ °C/W}$ ;  $\theta_{\text{conv}} = 18.3 \text{ °C/W}$ ), error is 9.47%. If  $h$  is  $1.704 \times 10^{-3} \frac{\text{W}}{\text{cm}^2 \text{ °C}}$ , error is 6.31%.

---

<sup>7</sup>This value represents the lower limit of the range of  $h$  usually encountered in natural convection, that is,  $h = 1 \text{ Btu/(hr)(ft}^2\text{)(°F)}$ .

## APPENDIX B

Functional Uncertainty Analysis

The functional uncertainty is a technique by which the uncertainties involved in the individual measurements of certain variables are combined to give an uncertainty representing the fractional uncertainty of the functional relationship which relates the variables.

Therefore the functional uncertainty is a systematic error since it is concerned only with the accuracy of the instruments. If the variables  $V_1$ ,  $V_2$  and  $V_3$  are related by the function  $R$ , that is,  $R = f(V_1, V_2, V_3)$ , the variation of the final reading can be written as a differential:

$$dR = \frac{\partial R}{\partial V_1} dV_1 + \frac{\partial R}{\partial V_2} dV_2 + \frac{\partial R}{\partial V_3} dV_3 \quad (B.1)$$

Define  $\omega_R$  as the standard deviation of the expected value of  $dR$ ,  $\omega_R = [E(dR^2)]^{1/2}$ , and assume:

$$E(dV_i dV_j) = 0, \quad i \neq j \quad (B.2)$$

Squaring Equation B.1 one will obtain:

$$\omega_R = \left[ \left( \frac{\partial R}{\partial V_1} \omega_{V_1} \right)^2 + \left( \frac{\partial R}{\partial V_2} \omega_{V_2} \right)^2 + \left( \frac{\partial R}{\partial V_3} \omega_{V_3} \right)^2 \right]^{1/2} \quad (B.3)$$

Dividing by  $R$  and letting  $\frac{V_1}{R} \frac{\partial R}{\partial V_1} = \frac{\partial \ln R}{\partial \ln V_1}$ , etc. the formula for the

fractional uncertainties is obtained:

$$\frac{\omega_R}{R} = \left[ \left( \frac{\partial \ln R}{\partial \ln V_1} \frac{\omega_{V_1}}{V_1} \right)^2 + \left( \frac{\partial \ln R}{\partial \ln V_2} \frac{\omega_{V_2}}{V_2} \right)^2 + \dots \right]^{1/2} \quad (\text{B.4})$$

Thus for a function of the form  $R = x^n y^{-p}$ ;

$$\frac{\omega_R}{R} = \left[ \left( \frac{n\omega_x}{x} \right)^2 + \left( \frac{-p\omega_y}{y} \right)^2 \right]^{1/2} \text{ while for a function of the form } Q = z+u,$$

$$\frac{\omega_Q}{Q} = \left[ \frac{\omega_z^2 + \omega_u^2}{(z+u)^2} \right]^{1/2}.$$

By using this procedure, functional uncertainty for the convective area of the heat sink with smallest diameter pins is found to be:

$$\frac{\omega_P}{P} = 0.00013 \text{ or } 0.013\%$$

and the functional uncertainty for the electric power (assuming no power losses) is:

$$\frac{\omega_P}{P} = 0.0037 \text{ or } 0.37\%$$

Based on these values,  $\frac{\omega_{q/A}}{q/A} = 0.0038 \text{ or } 0.38\%$  where  $q/A$  represents the heat flux input in the heat sink.

Considering the properties of the air exactly known and assuming a relationship of the type

$$Nu_D = K(Gr_D)^n$$

for finding the average Nusselt number, the functional uncertainty

analysis yields the accuracy of the heat transfer results. After some rearranging is done the above relationship becomes:

$$\frac{(D)(q/A)}{(\Delta T)} = K' (D^3 \Delta T)^n$$

or

$$K' = \frac{(q/A) D^{1-3n}}{(\Delta T)^{n+1}}$$

and finally, functional uncertainty is given by:

$$\frac{\omega_{K'}}{K'} = \left\{ \left[ (1-3n) \left( \frac{\omega_D}{D} \right) \right]^2 + \left( \frac{\omega_{q/A}}{q/A} \right)^2 + \left[ (-1-n) \left( \frac{\omega_{\Delta T}}{\Delta T} \right) \right]^2 \right\}^{1/2}$$

or, if considering n as having a representative value of 0.25,

$$\frac{\omega_{K'}}{K'} = 1.9\%.$$

## APPENDIX C

Combined Convection and Radiation Heat Transfer

The net radiation heat transfer rate between two gray surfaces is given by:

$$q_{1 \rightarrow 2} = A_1 \Omega_{1-2} (E_{b_1} - E_{b_2}) \quad (2.5)$$

$$\text{where } A_1 \Omega_{1-2} = \frac{1}{\frac{1-\epsilon_1}{A_1 \epsilon_1} + \frac{1}{A_1 F_{1-2}} + \frac{1-\epsilon_2}{A_2 \epsilon_2}}$$

In the case of a small body of surface area  $A_1$ , completely enclosed by a large area  $A_2$ , one could write  $F_{1-2} = 1.0$  and  $A_1/A_2 \ll 1$ . Therefore:

$$\Omega_{1-2} \approx \epsilon_1 \quad (C.1)$$

Substituting this in Equation 2.5 and using Equation 2.4, one obtains:

$$q_{1 \rightarrow \infty} = A_1 \epsilon_1 \sigma (T_1^4 - T_\infty^4) = A_1 \epsilon_1 \sigma (T_1 - T_\infty) (T_1^3 + T_1^2 T_\infty + T_1 T_\infty^2 + T_\infty^3) \quad (C.2)$$

where the reference temperature is considered to be the ambient temperature.



For small temperature differences:

$$T_1^3 + T_1^2 T_\infty + T_1 T_\infty^2 + T_\infty^3 \approx 4T^3 \quad ^7$$

$$\text{where } T = \frac{T_1 + T_\infty}{2}$$

Thus Equation C.2 becomes:

$$q_1 = h_r A_1 (T_1 - T_\infty) \quad (\text{C.3})$$

$$\text{where } h_r = \Delta \epsilon_1 \sigma T^3 \quad (\text{C.4})$$

is the radiation heat transfer coefficient.

The heat rate by convection and radiation is:

$$q_{\text{total}} = q_c + q_r \quad (\text{C.5})$$

Combining Equation C.5 with Equation C.3 and with Equation 2.7, the following is obtained:

$$h_{\text{total}} = h_c + h_r = \frac{q_{\text{total}}}{A_1 (T_1 - T_\infty)}$$

---

<sup>7</sup>This is a good assumption for this work since the error made is about half of one percent.

## APPENDIX D

Data Reduction Computer Program

```

      PROGRAM NUGR
C
C..THIS PROGRAM REDUCES DATA AND CALCULATES NUSSELT AND GRASHOF
C..NUMBERS AND THEIR LOGS..
C
      G=32.174
      DO 1 I=1,12
      K=I+12
      L=K+12
      READ(I,2) PD, AREA, D
      2 FORMAT(3F8.5)
      D=D/12.
      AREA=AREA/144.
      3 READ(I,7) POW, TINF, TWALL
      7 FORMAT(F7.4,F8.5,F9.5)
      IF(EOF(I)) GO TO 1
C
C..CALCULATE THE HEAT FLUX
C
      XQ=1.7065*POW/AREA
C
C..CONVERT EMF READINGS IN TEMPERATURE READINGS..
C
      TWALL=33.3908+34.7058*TWALL-0.14711*TWALL*TWALL
      TINF=33.3908+34.7058*TINF-0.14711*TINF*TINF
C
C..CALCULATE FILM TEMPERATURE..
C
      T=0.5*TWALL+0.5*TINF
C
C..CALCULATE AIR PROPERTIES..
C
      BETA=1./(TINF+460.)
      DENS=39.67417/(T+460.)
      VISC=9.81E-07*(0.5556*(T+460.))**1.5/(110.4+0.55560*
      $(T+460.))
      TK=0.00114*SQRT(T+460.)/(1.+10.**(-21.6/(T+460.))
      $441.7/(T+460.))
      DT=TWALL-TINF
      B=(DENS/VISC)*(DENS/VISC)
      XNUD=XQ*D/(TK*DT)
      GRD=G*BETA*DT*B*D**3
      GRP=GRD*PD**3
      XNUDLG=ALOG10(XNUD)
      GRDLG=ALOG10(GRD)
      GRPLG=ALOG10(GRP)
      WRITE(K,5) XNUDLG, GRDLG
      WRITE(L,5) XNUDLG, GRPLG
      5 FORMAT(2F10.5)
      WRITE(61,6) XNUDLG, GRDLG, GRPLG
      6 FORMAT(1X,3F10.5/)
      GO TO 3
      1 CONTINUE
      CALL EXIT
      END

```